Published in final edited form as:
Eur J Neurosci. 2011 December ; 34(11): 1767–1782. doi:10.1111/j.1460-9568.2011.07890.x.

The integrity of cholinergic basal forebrain neurons depends on expression of Nkx2-1

Lorenza Magno[1,*], **Oliver Kretz**[2], **Bettina Bert**[3], **Sara Ersözlü**[1], **Johannes Vogt**[4], **Heidrun Fink**[3], **Shioko Kimura**[5], **Angelika Vogt**[4], **Hannah Monyer**[4], **Robert Nitsch**[6,†], and **Thomas Naumann**[1,†]

[1]Institute of Cell Biology and Neurobiology, Centre of Anatomy, Charité Universitätsmedizin Berlin, Charitéplatz 1, 10117 Berlin, Germany

[2]Institute of Anatomy and Cell Biology, Centre for Neurosciences, Albert-Ludwigs-University of Freiburg, Freiburg, Germany

[3]Institute of Pharmacology and Toxicology, Department of Veterinary Medicine, Free University, Berlin, Germany

[4]Department of Clinical Neurobiology, University of Heidelberg, Heidelberg, Germany

[5]Laboratory of Metabolism, National Cancer Institute, National Institutes of Health, Bethesda, MD, USA

[6]Institute of Microanatomy and Neurobiology, University of Medicine, Johannes-Gutenberg-University Mainz, Mainz, Germany

Abstract

The transcription factor Nkx2-1 belongs to the homeobox-encoding family of proteins that have essential functions in prenatal brain development. Nkx2-1 is required for the specification of cortical interneurons and several neuronal subtypes of the ventral forebrain. Moreover, this transcription factor is involved in migratory processes by regulating the expression of guidance molecules. Interestingly, Nkx2-1 expression was recently detected in the mouse brain at postnatal stages. Using two transgenic mouse lines that allow prenatal or postnatal cell type-specific deletion of Nkx2-1, we show that continuous expression of the transcription factor is essential for the maturation and maintenance of cholinergic basal forebrain neurons in mice. Notably, prenatal deletion of Nkx2-1 in GAD67-expressing neurons leads to a nearly complete loss of cholinergic neurons and parvalbumin-containing GABAergic neurons in the basal forebrain. We also show that postnatal mutation of Nkx2-1 in choline acetyltransferase-expressing cells causes a striking reduction in their number. These degenerative changes are accompanied by partial denervation of their target structures and results in a discrete impairment of spatial memory.

Keywords

choline acetyltransferase; choreoathetosis; human; mouse; parvalbumin

Correspondence: Dr T. Naumann, as above. Thomas.Naumann@charite.de.
[†]R.N. and T.N. contributed equally to this work.
[*]*Present address*: Wolfson Institute for Biomedical Research, University College of London, London, UK.

Introduction

Mutations of homeobox genes expressed in the human forebrain may result in mental retardation, epilepsy and movement disorders (reviewed by Wigle & Eisenstat, 2008). For instance, haploinsufficiency of the transcription factor Nkx2-1 results in the so-called 'brain-thyroid-lung syndrome', a disease that emerges postnatally within the first few years of life (reviewed by Kleiner-Fisman & Lang, 2007). The prominent neurological symptoms include impairments of coordinated movements and a delayed development of speech (Breedveld *et al.*, 2002; Krude *et al.*, 2002). The specific symptoms suggest that the syndrome is caused by an abnormal development of the telencephalic parts of the basal ganglia (Krude *et al.*, 2002; do Carmo Costa *et al.*, 2005; Kleiner-Fisman & Lang, 2007).

During regionalization of the developing brain, multiple transcription factors are expressed in a specific temporal and spatial pattern (Schuurmans & Guillemot, 2002; Flames *et al.*, 2007). Among them, the homeobox gene *Nkx2-1* plays a critical role for cells generated in the hypothalamus and the medial ganglionic eminence (MGE), which contributes significantly to the development of various compartments of the telencephalon (Sussel *et al.*, 1999; Marin *et al.*, 2000; Garcia-Lopez *et al.*, 2008). For instance, MGE-derived neurons differentiate into GABAergic interneurons that migrate tangentially to the cortical mantle and the striatum, or integrate locally to form the lateral globus pallidus (LGP; Sussel *et al.*, 1999; Marin *et al.*, 2000; Butt *et al.*, 2005, 2008; Nobrega-Pereira *et al.*, 2010). In addition, Nkx2-1 exerts an important function in controlling the migration of postmitotic interneurons by regulating guidance receptors for semaphorins (Nobrega-Pereira *et al.*, 2008). In Nkx2-1 knockout mice, a substantial loss of cortical interneurons was observed together with severe morphological alterations of the striatum and various nuclei of the diencephalon (Kimura *et al.*, 1996), whereas the gross brain morphology was described as normal for Nkx2-$1^{+/-}$ mice (Pohlenz *et al.*, 2002). In addition, it has been shown that a postnatal synapsin I-driven deletion of the *Nkx2-1* gene led to various vegetative dysfunctions (for reviews, see Son *et al.*, 2003; Kim *et al.*, 2006) due to alterations in the hypothalamus. However, no morphological or behavioural impairments were found in these conditional mutant mice that could be associated with telencephalic structures (Mastronardi *et al.*, 2006).

Recently we showed that, predominantly, choline acetyltransferase (ChAT)-expressing neurons and parvalbumin (PV)-positive GABAergic neurons of the ventral forebrain maintain synthesis of Nkx2-1 throughout life (Magno *et al.*, 2009). These findings, as well as the postnatal onset of neurological symptoms in humans, suggest that Nkx2-1 not only acts during prenatal brain development, but may also be needed for the postnatal maturation and maintenance of these neurons. We therefore generated mouse lines with cell type-specific ablation of *Nkx2-1* during embryonic or postnatal development. Our results show that both prenatal and postnatal expression of Nkx2-1 is required for the maintenance of cholinergic basal forebrain neurons and their projections.

Materials and methods

Mouse lines, generation of conditional mice and genotyping

Mice expressing Cre-recombinase under the *GAD67*-promoter ($GAD^{cre/+}$) were kindly provided by H. Monyer (Heidelberg, Germany). The targeting vector used for generating these mice contained a fragment of the murine *GAD67* gene spanning parts of exon 1 up to intron 6. The Cre-recombinase cDNA was placed 30 bp upstream of the translational start codon of *GAD67*, so that protein expression is driven by *GAD67.*

B6;129S6-*Chattm1(cre)Lowl/J* mice ($ChAT^{cre/+}$) were purchased from Jackson Laboratories (Charles River, Sulzfeld, Germany; stock number 6410*).* In these mice, Cre-recombinase

expression is controlled by the endogenous gene promoter. The targeting vector was designed to insert an internal ribosome entry site-linked Cre recombinase gene (IRES-Cre) downstream of the stop codon of the *ChAT* gene. ChAT expression was described to be unaffected and Cre-recombinase activity was reported for all cholinergic neurons (Jackson Laboratories). The two knock-in mice were first bred with C57Bl/6 mice to obtain a uniform genetic background. Nkx2-1^{tm2Shk} mice (*Nkx2-1$^{fl/fl}$*) have been described in detail previously (Kusakabe *et al.*, 2006).

To generate conditional mice with the *Nkx2-1* deletion, the two Cre-lines were crossed with *Nkx2-1$^{fl/fl}$* mice. Subsequently, Cre-positive mice of the F1 generation were bred with the homozygous floxed mice in order to delete *Nkx2-1* in GAD67- and ChAT-positive cells, respectively.

The two Cre-lines and the mutants (*GAD$^{cre/+}$;Nkx2-1$^{fl/fl}$* and *ChAT$^{cre/+}$;Nkx2-1$^{fl/fl}$*) were also crossed with homozygous B6;129S4-*Gt(ROSA)26Sor^{tm1Sor}/J mice (also known as ROSA26*-LacZ reporter line; kindly provided by G. Willimsky, CBF, Berlin) to generate *GAD$^{cre/+}$;R26R*, *ChAT$^{cre/+}$;R26R*, *GAD$^{cre/+}$;R26R; Nkx2-1$^{fl/fl}$* and *ChAT$^{cre/+}$;R26R;Nkx2-1$^{fl/fl}$* mice.

All animals were housed on a 12/12-h light/dark cycle with access to food and water *ad libitum* and in accordance with institutional guidelines for animal welfare. Behavioural tests were performed according to the state authority of Berlin, Landesamt für Gesundheit und Soziales (LAGeSo; permit no. G 0004/09). The number of animals used for the different approaches, including their various survival times, is provided in the relevant sections of the results.

Mouse-tail biopsies were digested and processed by using an Invisorb Spin Tissue Mini kit (Invitek GmbH, Berlin, Germany). The following primers and annealing temperatures (T_a) were used to detect the Cre or floxed constructs in the genome – GAD67-Cre primers (designed by A. Vogt, Heidelberg, Germany) 5′-CCGGCGCCCCTTAGCTGTGAG-3′ and 5′-GGTTCTTGCGAACCT-CAT-CACTCG-3′ (T_a = 63 °C); ChAT-Cre primers (designed by Jackson Laboratories) 5′-GTTTGCA-GAAGCGGTGGG-3′, 5′-AGATAG-ATAATGAGAGGCTC-3′ and 5′-CCTTCTATCGCCTTCTTGACG-3′ (T_a = 55 °C); Nkx2-1-floxed primers (two Neo primers previously described by Kusakabe *et al.*, 2006); internal primer designed by K. Paulick (MDC, Berlin-Buch) – 5′-TGCCGTGTAAACACGAGGAC-3′, 5′-GACTCTCAAGCAAGTC-CATCC-3′ and 5′-GAAGTGGCGAAAGCTAC-AGG-3′ (T_a = 55 °C).

The PCR conditions consisted of an initial activation step of 5 min at 95 °C and 35 cycles of 30 s of denaturation at 94 °C, 30 s of annealing (see above for specific T_a), and 30 or 40 s extension at 72 °C, and a final extension of 5 min at 72 °C.

Human tissue

We investigated tissue of the basal ganglia of two human brains from routine autopsies (males – 21 and 42 years old). The samples were obtained in accordance with local ethical committee guidelines. The subjects died of non-neurological causes.

The samples were sliced fresh into thick slabs (1 cm), frozen in liquid nitrogen and then stored at −80 °C. The slabs containing parts of the basal ganglia were cut with the cryostat into 100-μm-thick coronal sections that were serially collected in cold 0.1 M phosphate buffer.

Histochemistry and immunofluorescence

Brains of E14.5 and E16.5 embryos and newborns were dissected out of the skull and fixed overnight by immersion in a fixative containing 4% paraformaldehyde (PFA) and 0.1% glutaraldehyde in 0.1% phosphate buffer (PB). For fine-structural analysis the brains were further processed as described below.

All other animals (from P2 onward) assigned to morphological analyses were anaesthetized and transcardially perfused with 4% PFA in PB as described in detail (Magno *et al.*, 2009). Animals assigned to X-gal staining were perfused with a fixative containing 4% PFA and 0.2% glutaraldehyde in PB. The brains were subsequently cut coronally (E14.5 to P2 – 100 μm; all others – 50 μm) on a vibratome and the sections were stored in PB. After treatment with 0.6% H_2O_2 in 0.1 M PB for 20 min, the 'free floating' sections were pre-incubated in a solution containing 5 or 10% normal serum of the species in which the secondary antibody was raised (see secondary antibodies below), 5% bovine serum albumin, and 0.2% Triton-X in 0.1 M PB for 1 h at room temperature. After incubation with primary antibodies (see below) the sections were transferred to solutions containing biotinylated goat anti-rabbit IgG (for PV, Nkx2-1, NeuN, $p75^{NTR}$), biotinylated rabbit anti-rat IgG (for somatostatin, SOM), or biotinylated rat anti-goat IgG (for ChAT; all secondary antibodies –Vector Laboratories, Burlingame, CA, USA), diluted 1 : 250 in PB for 2 h at room temperature. Subsequent visualization of the labelling by ABC (1 : 250, Elite Vectastain ABC kit; Vector Laboratories) and DAB reactions was performed as described previously (Magno *et al.*, 2009).

Immunofluorescence (IF) stainings were used for labelling of sections obtained from the two human brains and for double-labelling for β-galactosidase (β-gal) and ChAT or PV. These sections were labelled with primary antibodies (see below) and visualized with AlexaFluor 488- and AlexaFluor 568-conjugated secondary antibodies (Invitrogen, Karlsruhe, Germany), mounted on slides and coverslipped with DAKO fluorescent mounting medium.

For immunohistochemistry (IHC) and IF we used the following primary antibodies – polyclonal rabbit anti-PV (1 : 5000, IHC) and monoclonal rabbit anti-PV (1 : 500, IF; both from Swant, Bellinzona, Switzerland), polyclonal goat anti-ChAT (1 : 100, IHC; 1 : 500, IF) and monoclonal mouse anti-GAD67 (1 : 1000, IF; both from Chem-icon International, Temecula, CA, USA), polyclonal anti-$p75^{NTR}$ (1 : 1000; Promega, Madison, WI, USA), polyclonal anti-β-gal (1 : 3000; ICN/Cappel, Durham, NC, USA), polyclonal anti-TTF1 (1 : 2000, IHC; 1 : 500, IF; Santa Cruz Biotechnology, Santa Cruz, CA, USA), and monoclonal mouse anti-NeuN (1 : 1000, IHC and IF; Chemicon).

The extent of the loss of cholinergic fibres in the mutant mice was examined using acetylcholine esterase (AChE)-histochemistry according to previous protocols (Eckenstein & Sofroniew, 1983; see Kermer *et al.*, 1995). In addition, axons of the cholinergic basal forebrain neurons were also analysed in sections immunolabelled with antibodies against ChAT or $p75^{NTR}$ (see above).

5-Bromo-4-chloro-3-indolyl-β-D-galactosidase (X-gal) staining was performed as follows. Immediately prior to staining, free-floating sections were re-fixed in 0.2% glutaraldehyde for 10 min on ice, rinsed in PB and then incubated in detergent solution (0.02% Igepal, 0.01% sodium deoxycholate and 2 mM $MgCl_2$ in PB) for 10 min. The sections were directly transferred into the staining solution [5 mM $K_4Fe(CN)_6$, 5 mM $K_3Fe(CN)_6$, 2 mM $MgCl_2$, 1 mg/mL X-gal in dimethylformamide, in 1× PBS] and subsequently incubated at 37 °C overnight. Thereafter, the slides were fixed in 4% PFA for 10 min. After rinsing in PB the sections were further processed for ChAT- or PV-IHC as described above and subsequently mounted on slides and coverslipped.

Stereological cell counts

Stereological cell counts (Stereo Investigator software version 4.31 – MicroBrightField, Inc., Williston, VT, USA) were performed for ChAT- and PV-immunoreactive (ir) neurons in the medial septum-vertical limb of the diagonal band complex (MSvDB), the horizontal limb of the diagonal band-substantia innominata (hDB-SI), the caudate-putamen (CPu) and the LGP. For the LGP, total neuronal cell numbers and total volume were additionally estimated by using IHC for NeuN. The optical disector/fractionator method was applied for the various regions as described in detail previously (Naumann *et al.*, 2002). A smaller frame size (30 × 18 μm) was used for estimation of the numbers of NeuN-positive cells in the LGP. Volume calculation for the LGP was based on the following parameters –region investigated (LGP), number of sections and section thicknesses. Cell numbers of the various nuclei represent data obtained for one side of the brain.

Fine-structural analysis

Some of the brains were used for fine-structural analysis. Embryonic brains were processed as described above. Transcardial perfusion of postnatal mice was performed by using a fixative containing 4% PFA and 0.1% glutaraldehyde in 0.1 M PB. Immunocytochemical labelling of neurons and subsequent tissue handling for electron microscopy was performed as described in detail by Magno *et al.* (2009). Embedded tissue blocks underwent semi-thin sectioning (1–2 μm thickness) followed by ultrathin sectioning. All cuts were performed on a Reichert Ultracut S. The ultrathin sections were examined using a Zeiss EM 900 electron microscope.

In situ hybridization combined with immunohistochemistry

In situ hybridization (ISH) was performed for the transcription factors *Nkx2-1* (Magno *et al.*, 2009), *Lhx7* (the digoxigenin-labelled RNA probe was kindly provided by G. Fishell, New York, USA) and *Lhx6* (the digoxigenin-labelled RNA probe was kindly provided by V. Pachnis, London, UK; for detailed protocols see Magno *et al.*, 2009). Hybridization was performed overnight at 60 °C. Some of the sections were subsequently immunostained for Nkx2-1 or SOM (1 : 2500, Chemicon) as described in detail previously (Magno *et al.*, 2009).

Image processing

Images were captured using an Olympus digital camera (Olympus BX-51, Hamburg, Germany). Fluorescent images were obtained with a Leica confocal laser-scanning microscope. They were then processed with Adobe Photoshop CS3 (Adobe Systems Inc., San Jose, CA, USA) for general contrast and brightness enhancements and colour-level adjustments, and finally handled with Adobe Illustrator CS3 (Adobe Systems Inc.) for final compositing of the figures.

Real-time PCR

Mice used for RNA extraction were culled by cervical dislocation and the brains were stored at −80 °C until use. Total RNA was isolated from the forebrains and reverse transcribed as described previously (Magno *et al.*, 2009). *NGF*, *trkA*, $p75^{NTR}$, *trkB* as well as two housekeeping genes (*HPRT* and *GAPDH*) were measured with TaqMan Gene Expression Assays on an ABI PRISM 7500 Fast real-time PCR detection system (Applied Biosystems Inc., Foster City, CA, USA). To validate the amplification efficiency of the various assays, standard curves were generated. As normalization to the endogenous control genes *HPRT* and *GAPDH* led to similar results, we present only the data normalized to *GAPDH* expression.

Results for relative gene expression were calculated using the $2^{-\Delta CT}$ method. Universal TaqMan master mix was purchased from Applied Biosystems and used according to the manufacturer's recommendations.

Behavioural tests

The Morris water maze (MWM) experiment was performed according to Bert *et al.* (2005). Briefly, the test was performed over 11 days and consisted of an adaptation trial (day 0), 8 days for the place version (days 1–8), the spatial probe (day 9) and the cued version (day 10). The performances were recorded by using a computerized tracking system (VideoMot version 2.3; TSE Systems, Bad Homburg, Germany). In addition, swim path (in cm) was measured and average speed was calculated (cm/s). Two weeks after the MWM test, the animals were tested on an accelerating rota-rod (Ugo Basile, Comerio, Italy) as already described in detail for rats (Bert *et al.*, 2002).

Statistical analysis

Differences between the experimental groups (cell counts, real-time PCR) were determined by two-tailed unpaired Student's *t*-tests with confidence intervals of 95% and were considered significant at $P < 0.05$. *P*, *t* ratio and degrees of freedom are reported for each test. All calculations were performed with GraphPad Prism version 4.00 for Microsoft Windows (GraphPad Software, San Diego, CA, USA).

As the behavioural data were not normally distributed (tested by the Shapiro–Wilk's method) non-parametric tests were generally chosen. MWM data were analysed using Friedman one-way ANOVAs by ranks followed by *post-hoc* Dunnett's method (place version, each group was analysed separately) and by Mann–Whitney rank-sum tests to detect differences between genotypes for each day of the place version and for each trial of the cued version. For the spatial probe, the time in the former platform quadrant (PQ) was compared with the mean of the three remaining quadrants (MQ) and was analysed by Wilcoxon matched-pairs tests. Data of the rota-rod test were analysed by Mann–Whitney rank-sum tests. All analyses were performed with Sigma-Plot version 11.0 (Systat Software Inc., Chicago, IL, USA). A difference was considered statistically significant at *P* (two-tailed) < 0.05.

Results

The transcription factor Nkx2-1 is expressed in many cholinergic and PV-positive GABAergic neurons throughout the ventral forebrain (Magno *et al.*, 2009). We therefore examined the effects of *Nkx2-1* deletion on these cell populations following GAD67-driven inactivation of the transcription factor (prenatal deletion, referred to as – $GAD^{cre/+};Nkx2\text{-}1^{fl/fl}$), and after ChAT-induced inactivation of the gene (postnatal deletion, referred to as – $ChAT^{cre/+};Nkx2\text{-}1^{fl/fl}$) and compared these data with those obtained from the two genotypes which served as controls – $Nkx2\text{-}1^{fl/fl}$, as well as $GAD^{cre/+};Nkx2\text{-}1^{fl/+}$ and $ChAT^{cre/+};Nkx2\text{-}1^{fl/+}$. However, as no significant differences were found between the two controls regarding cell numbers, axonal pattern and performances in the behavioural tests, we largely present results obtained from the two $Nkx2\text{-}1^{fl/fl}$ animal lines as control values.

Cre-recombinase activity in GAD67- and ChAT-immunoreactive neurons of the forebrain

We first characterized Cre-recombinase activity in the two mouse lines by crossing them with the Cre-reporter ROSA26LacZ (*R26R*). Transcripts for *GAD67* have been found as early as embryonic day (E)10 and, shortly thereafter, in the differentiation zones of the ventral forebrain (Katarova *et al.*, 2000). Accordingly, in $GAD^{cre/+};R26R$ mice the typical 'bluish' reaction product of the X-gal staining was already observed in the prenatal forebrain

long before proteins such as ChAT and PV become upregulated. As shown at postnatal day (P)2, X-gal staining could be detected in many regions of the differentiated ventral forebrain, including the CPu and septal complex (Fig. 1A and B, respectively). Throughout the subcortical brain, a dense, punctuate-like labelling was observed, which corresponds to the density of GABAergic neurons in these regions (cf. Bender *et al.*, 1996; Magno *et al.*, 2009).

Cholinergic and GABAergic interneurons were described to develop from common proto-GABAergic precursors, at least in the striatum (Fragkouli *et al.*, 2009b). Hence, at P8 the X-gal-labelled cells could be identified as PV-immunoreactive (PV-ir; not shown), but also as ChAT-ir neurons (Fig. 1C and D) in the $GAD^{cre/+};R26R$ mice. Close inspection of the sections revealed that the majority of these two neuronal cell types contained the activity of this Cre-driver, as demonstrated by the presence X-gal labelling in these cells (Fig. 1C and D).

Several studies performed in rodents have shown that ChAT synthesis is switched on around P4/5 and reaches mature expression levels around P15 (Korsching, 1993; Bender *et al.*, 1996; Naumann *et al.*, 2002). Consistent with this, no X-gal precipitates were found until P3/4 in $ChAT^{cre/+};R26R$ mice (Fig. 1E). Similar stainings performed at P8 resulted in strong labelling of cellular profiles. The density of these cells resembled that of the adult staining pattern for cholinergic neurons. As shown for the MSvDB (Fig. 1F and G), hDB-SI (Fig. 1H) and CPu (Fig. 1I), most of the cells could be identified as ChAT-ir neurons. Similar to the observations made for the $GAD^{cre/+};R26R$ mice, only a small subset of cholinergic neurons did not contain precipitates of the X-gal reaction (cf. Fig. 1G and H). To confirm that Cre activity is restricted to the cholinergic population, we performed double immunofluorescence stainings for β-gal and PV. As shown for the CPu, no co-localization of the two markers could be detected, suggesting that Cre activity is not ectopically present in non-cholinergic cells (Fig. 1J).

Deletion of Nkx2-1 leads to substantial loss of ChAT- and PV-ir neurons in the basal forebrain

We next studied the consequences of Nkx2-1 deletion on the number of cholinergic and PV-positive neurons of the MSvDB, hDB-SI, CPu and LGP by using the optical disector/fractionator method (West *et al.*, 1991; cf. Naumann *et al.*, 2002). The regions of interest (described in Fig. 2P) for the cell counts are shown for three different levels of the rostro-caudal extension of the brain (modified from Paxinos, 2001).

Cell counts revealed a dramatic decrease of the two cell populations in $GAD^{cre/+};Nkx2\text{-}1^{fl/fl}$ mutant mice at 3 months of age compared with age-matched controls ($n = 7$ each; two-tailed unpaired Student's t-test, d.f. = 12; Fig. 2A–J; Table 1). Loss of neurons was found to be most prominent in the CPu (PV: −93.1%, $P < 0.0001$, $t = 28.49$; ChAT: −98.6%, $P < 0.0001$, $t = 16.13$). A comparable cell loss was detected in the MSvDB (PV: −50%, $P = 0.0017$, $t = 4.021$; ChAT: −79.1%, $P < 0.0001$, $t = 6.935$), the hDB-SI (PV: −79.5%, $P < 0.0001$, $t = 10.86$; ChAT: −84%, $P < 0.0001$, $t = 9.533$), and the LGP (PV: −77.7%, $P < 0.0001$, $t = 13.06$; ChAT: −52.6%, $P < 0.0001$, $t = 6.947$). We also performed corresponding cell counts on $GAD^{cre/+};Nkx2\text{-}1^{fl/fl}$ animals at P15. However, the cell numbers of PV- and ChAT-ir neurons were reduced already at this age (data not shown) and corresponded to that of 3-month-old mutants.

We then analysed the number of cholinergic neurons in the various regions of interest in $ChAT^{cre/+;}Nkx2\text{-}1^{fl/fl}$ mice and in the two controls ($Nkx2\text{-}1^{fl/fl}$ and $ChAT^{cre/+};Nkx2\text{-}1^{fl/+}$; Fig. 2K–O). At 3 months of age the number of ChAT-ir neurons (Table 2; Fig. 2K–O) was significantly reduced to about 50% in $ChAT^{cre/+};Nkx2\text{-}1^{fl/fl}$ mice compared with that of

Nkx2-1$^{fl/fl}$ controls (n = 6 each, two-tailed unpaired Student's t-test, d.f. = 10; MSvDB: −50.2%, P = 0.0005, t = 5.026; hDB-SI: −45.4%, P = 0.0016, t = 4.268; CPu: −52.7%, P < 0.0001, t = 8.286; LGP: −62.2%, P < 0.0001, t = 6.316).

To investigate the onset and progression of the cell loss in more detail, we performed additional stereological cell counts for P15 (mutants – n = 6, controls – n = 4) and 6-month-old (n = 5 each) animals (Fig. 2K). No differences in cell numbers were observed between *Nkx2-1*$^{fl/fl}$ and *ChAT*$^{cre/+}$*;Nkx2-1*$^{fl/fl}$ mice at P15 (two-tailed unpaired Student's t-test, d.f. = 8; MSvDB – P = 0.4613, t = 0.773; hDB-SI – P = 0.9283, t = 0.092; CPu – P = 0.9928, t = 0.009; LGP – P = 0.8549, t = 0.188; Table 2; Fig. 2K; cf. Naumann *et al.*, 2002). Interestingly, no evidence for a progressive loss of ChAT-ir neurons in mutant mice was detected between 3 months (see above) and 6 months of age (Fig. 2K, Table 2).

To verify the specificity of the postnatal mutation of Nkx2-1 in cholinergic neurons, we also performed cell counts for PV-ir neurons in *ChAT*$^{cre/+}$*;Nkx2-1*$^{fl/fl}$ and *Nkx2-1*$^{fl/fl}$ mice. However, no alteration of this subset of GABAergic neurons was observed in the various regions of interest (data not shown). This is consistent with the lack of Cre-recombinase activity in these neurons (see above).

Inactivation of the Nkx2-1 gene leads to degenerative changes in basal forebrain neurons

In the rodent brain, many subcortical regions including the large ventral magnocellular nuclei differentiate between E13 and 18 (e.g. Bayer, 1979). The efficiency of the genetic manipulation was therefore monitored in the ventral forebrain of *GAD*$^{cre/+}$*;Nkx2-1*$^{fl/fl}$ mice by using IHC and ISH for Nkx2-1 at prenatal and postnatal stages.

Conditional prenatal *Nkx2-1* ablation in GAD67-expressing cells resulted in an almost complete loss of Nkx2-1-ir cells in the various subcortical compartments of *GAD*$^{cre/+}$*;Nkx2-1*$^{fl/fl}$ mice even at prenatal stages (cf. Fig. 3A and B). As shown at E16.5, only at the level of the ventricular zone of the lateral ventricles a persistent synthesis of the transcription factor was observed (Fig. 3B). Away from the ventricular region, Nkx2-1 expression tends to fade gradually, suggesting that the mutation occurs as the cells exiting their cycle start to express GAD67 (Fig. 3C).

The reduction in cell numbers as observed for the *GAD*$^{cre/+}$*;Nkx2-1*$^{fl/fl}$ mice (see above) could be caused by different processes occurring in the mutated cells. For instance, it has been described that *Nkx2-1* ablation in the MGE at early prenatal stages may result in a shift of the molecular profile of the mutated cells (Butt *et al.*, 2008), or in an alteration of their migratory capacity (Nobrega-Pereira *et al.*, 2008). Thus, a fine-structural analysis of tissue samples obtained from the ventricular zone at E14.5 was performed for *GAD*$^{cre/+}$*;Nkx2-1*$^{fl/fl}$ mice and corresponding controls (Fig. 3C and D). At this age, large accumulations of cell profiles showing severe signs of degeneration and cell debris were detectable (Fig. 3E and F), which were not observed for corresponding control animals (Fig. 3D). In these electron-dense structures, cell organelles including the cell nucleus could hardly be detected (Fig. 3E and F). Subsequent fine-structural investigation of the LGP or other subcortical compartments including the MSvDB of *GAD*$^{cre/+}$*;Nkx2-1*$^{fl/fl}$ animals at 1 or 3 months of age did not provide evidence for a degeneration of neurons (data not shown). Taken together, these data do not support the hypothesis that mutated neurons differentiate into another phenotype, but rather suggest that they degenerate locally.

To confirm further that Nkx2-1-expressing cells are not replaced by other cell types, we determined the total volume and number of neurons of the LGP, a structure known for its very high number of neurons expressing both PV and Nkx2-1 (Magno *et al.*, 2009; Nobrega-Pereira *et al.*, 2010). Close inspection of slices processed for IHC already indicated that the

LGP of *GAD*$^{cre/+}$;*Nkx2-1*$^{fl/fl}$ mice was significantly smaller in size. Accordingly, both the total volume (Fig. 3G, right; $n = 6$ each, two-tailed unpaired Student's *t*-test, d.f. = 10; *GAD*$^{cre/+}$;*Nkx2-1*$^{fl/fl}$ = 0.51 mm^3 vs. *Nkx2-1*$^{fl/fl}$ = 0.97 mm^3; −47.6% $P < 0.0001$, $t = 6.645$) and the total number of NeuN-positive neurons (Fig. 3G, left; $n = 3$ each, two-tailed unpaired Student's *t*-test, d.f. = 4; *GAD*$^{cre/+}$;*Nkx2-1*$^{fl/fl}$ = 3146.3 vs. *Nkx2-1*$^{fl/fl}$ = 7543.3; −58.3% $P = 0.0015$, $t = 7.735$) of the mutated LGP were substantially reduced compared with controls. Thus, this region was obviously not populated by other neuronal cell types after deletion of Nkx2-1.

Developing cholinergic and GABAergic basal forebrain neurons can be further characterized by the expression of transcription factors acting downstream of Nkx2-1, namely Lhx7 and Lhx6 (Sussel *et al.*, 1999; Du *et al.*, 2008). As shown for the CPu of *GAD*$^{cre/+}$;*Nkx2-1*$^{fl/fl}$ mutants at 3 months of age, no cells positive for either *Lhx7* mRNA or Nkx2-1 could be detected (cf. Fig. 3H–J). A similar loss of cholinergic neurons was observed in the neighbouring regions, including the septal complex and the LGP (data not shown). In contrast, *Lhx6* labelling was found to be partially maintained in the CPu of mutant mice (Fig. 3M), and most Lhx6-positive cells could be double-labelled by subsequent IHC for SOM (Fig. 3N). SOM-positive striatal neurons are known to downregulate Nkx2-1 expression as soon as they exit their cell cycle (Marin *et al.*, 2000), and they are therefore not affected by the mutation. These data also point to the possibility that prenatal deletion of Nkx2-1 in postmitotic cells leads to their degeneration rather than causing cell-fate shift and/or migratory defects.

The cholinergic phenotype of ventral forebrain neurons develops within the first 2 weeks after birth (Gnahn *et al.*, 1983; Mobley *et al.*, 1986; Sofroniew *et al.*, 1987), and mature cell numbers are detectable around P12–15 (cf. Bender *et al.*, 1996; Naumann *et al.*, 2002). As shown by our cell counts, in postnatal *ChAT*$^{cre/+}$;*Nkx2-1*$^{fl/fl}$ mice a substantial loss of cholinergic basal forebrain neurons was detected at 3 months of age. These changes were therefore preferentially examined by using fine-structural methods. Among the neurons lacking signs of degeneration (cf. Fig. 4A and B) we found a large number of very dark-coloured neurons in semi-thin tissue preparations (Fig. 4B). At ultrastructural level, these cells appeared electron-dense and thus organelles and membranes could barely be detected (cf. Fig. 4C–E). However, many of these neurons still present intact nuclear membranes and, at least partially, input synapses (Fig. 4E). These fine-structural characteristics indicate long-lasting degenerative processes rather than apoptotic cell death (cf. Naumann *et al.*, 1992b). As revealed by the cell counts for *ChAT*$^{cre/+}$;*Nkx2-1*$^{fl/fl}$ mice (Fig. 2K), about 50% of the ChAT-ir neurons remain detectable after ChAT-Cre driven ablation of Nkx2-1. These cells do not show signs of degeneration and, as shown for the CPu, they do not express Nkx2-1, at least during the various postnatal stages analysed (Fig. 4F). By using confocal microscopy, subsequent analysis of cells in the forebrain of *ChAT*$^{cre/+}$;*R26R*;*Nkx2-1*$^{fl/fl}$ mice revealed that almost all remaining ChAT-positive neurons were also labelled for β-gal (Fig. 4G–I).

Target denervation and altered expression of neurotrophin receptors in Nkx2-1-deficient mice

By using histochemistry for AChE (Eckenstein & Sofroniew, 1983; Mesulam *et al.*, 1983), we next investigated whether the loss of cholinergic neurons in the two mouse lines is accompanied by corresponding impairment of their axonal projections. At 3 months of age, a nearly complete absence of AChE-positive fibres was observed throughout the cortical mantle (Fig. 5A and B) including the hippocampal formation (Fig. 5E and F), and within the CPu (Fig. 5I and J) of *GAD*$^{cre/+}$;*Nkx2-1*$^{fl/fl}$ mutants. Notably, the AChE labelling of fibres was similarly impaired in the mutants at 2 and 4 weeks of age (data not shown). Only in

more latero-ventral parts of the cortex (e.g. in the piriform cortex and the amygdaloid complex) did the AChE staining pattern appear to be unchanged (data not shown).

In *ChAT$^{cre/+}$;Nkx2-1$^{fl/fl}$* mice similar alterations of the AChE staining were observed in the neocortex at 3 months of age. Only a few aberrant fibres, mostly located in superficial and deep parts of the neocortex, were detected (Fig. 5C and D). Surprisingly, the AChE-staining pattern was better preserved in the CPu and in the hippocampus proper. As shown for the granule cell layer of the dentate gyrus, the AChE pattern exhibited defects in a 'patch-like' manner (cf. Fig. 5G and H). Alternative labelling of cholinergic projections by using antibodies against ChAT or p75^{NTR}, the latter known to be a specific marker for the cholinergic magnocellular projections (Sobreviela *et al.*, 1994), resulted in an identical staining pattern (data not shown), which confirms our results obtained from the AChE stainings.

In conclusion, following prenatal mutation of Nkx2-1, an extensive loss of cholinergic fibres was observed in all regions studied. On the other hand, postnatal ablation of the transcription factor is also accompanied by an extensive loss of cholinergic terminals in large parts of the neocortex, but was found to be less pronounced in other regions including the basal ganglia and the allocortical hippocampal formation.

Neurotrophins and their receptors are known to be of considerable importance for the differentiation, maturation and maintenance of cholinergic basal forebrain neurons (Li *et al.*, 1995; Thoenen, 1995; Yoon *et al.*, 1998; Bibel & Barde, 2000; Sofroniew *et al.*, 2001). We therefore investigated whether the cellular changes observed in the mutants at 3 months of age are accompanied by impaired synthesis of these molecules. However, no significant differences were detected for the level of nerve growth factor (*NGF)* between the mutants and their corresponding controls ($n = 5$ each, two-tailed unpaired Student's t-test, d.f. = 8; *GAD$^{cre/+}$;Nkx2-1$^{fl/fl}$* vs. *Nkx2-1$^{fl/fl}$* $P = 0.6872$, $t = 0.4176$; *ChAT$^{cre/+}$;Nkx2-1$^{fl/fl}$* vs. *Nkx2-1$^{fl/fl}$* $P = 0.4262$, $t = 0.8384$; Fig. 5K and L). In contrast, significant decreases in the expression of *trkA* (−82%, $P = 0.01$, $t = 3.353$) and *p75^{NTR}* (−60%, $P = 0.0006$, $t = 5.477$) transcripts were detected for *GAD$^{cre/+}$;Nkx2-1$^{fl/fl}$* mice (Fig. 5K), whereas in *ChAT$^{cre/+}$;Nkx2-1$^{fl/fl}$* mutants a significant reduction was only observed for *trkA* (−56%, $P < 0.0001$, $t = 5.497$; *p75^{NTR}*: −41% $P = 0.0887$, $t = 1.937$; Fig. 5L). We also tested whether trkB, known to be involved in the brain-derived neurotrophic factor-mediated effects on GABAergic striatal neurons (e.g. Mizuno *et al.*, 1994; Reichardt, 2006), was regulated after targeting of *Nkx2-1.* Again, no significant differences could be detected between the animal groups regarding the levels of this neurotrophin receptor (data not shown). These results additionally confirm that in both mutations the cholinergic basal forebrain neurons are heavily impaired despite relevant synthesis of NGF (cf. Rocamora *et al.*, 1996; McAllister *et al.*, 1999).

Behavioural impairments following ablation of Nkx2-1

Any substantial loss of cholinergic and GABAergic neurons of the ventral forebrain might be accompanied by impairments of the motor/cognitive behaviour (e.g. Arters *et al.*, 1998; Berger-Sweeney, 2003; Bonsi *et al.*, 2011). Accordingly, *GAD$^{cre/+}$;Nkx2-1$^{fl/fl}$* mice of both sexes showed significant deficits in the place version of the MWM task (Fig. 6A). Female mutant mice failed to learn the location of the platform [$\chi^2_7 = 11.03$ ($n = 7$), $P = 0.137$], whereas their corresponding controls learned the task, as shown by progressively decreasing escape latencies from day 3 onwards [$\chi^2_7 = 25.70$ ($n = 7$), $P < 0.001$; followed by Dunnett's method; Fig. 6A, left]. Detailed analysis by Mann–Whitney rank sum-tests of each day revealed that, during all 8 days of the test, female *GAD$^{cre/+}$;Nkx2-1$^{fl/fl}$* mice showed significantly higher escape latencies than female control mice (see Fig. 6A, left).

Additionally, the swimming paths of female mutants were significantly longer (Fig. 6D) and average speed slightly lower compared with female control mice (data not shown). The learning deficit was reflected by the spatial probe after removing the platform. Female $GAD^{cre/+};Nkx2\text{-}1^{fl/fl}$ mice spent similar swimming times in all quadrants ($P = 0.938$), but female control mice also displayed equal swimming times in all quadrants ($P = 0.156$; Fig. 6B). In the cued version, female mutant mice displayed in two trials longer escape latencies than female control mice, pointing to disturbed visual-motor integrity or reduced overall learning capacity (Fig. 6A, left).

Male mutant mice showed no significant decreases in escape latencies during the place version of the MWM [$\chi^2_7=12.39$ ($n = 7$), $P = 0.089$], whereas male control mice learned to locate the platform [$\chi^2_7=18.45$ ($n = 7$), $P = 0.010$; Fig. 6A, right]. Day-by-day comparison of the performances by Mann–Whitney rank sum-tests revealed significant differences between mutant and controls for days 6 and 8 (see Fig. 6A, right). The swimming speed was only slightly lower in male mutant mice than in male control mice, whereas no differences in the swim path length were observed between both genotypes (data not shown). The spatial probe trial revealed that both male control ($P = 0.078$) and $GAD^{cre/+};Nkx2\text{-}1^{fl/fl}$ mice ($P = 0.813$) were not able to remember the former platform location (Fig. 6B). It is possible that the learning and memory impairment of male mutant mice is due either to general learning deficits or deficits in vision/motor activity as suggested by the results of the cued version (Fig. 6A, right).

The deficits in visual-motor integrity of $GAD^{cre/+};Nkx2\text{-}1^{fl/fl}$ mice of both sexes observed during the cued version of the MWM are reflected in the rota-rod test, a frequently applied test for detecting disturbances of subcortical organization of motor functions (Bert *et al.*, 2002). Male ($t_6 = 30.00$, $P = 0.002$) and female ($t_6 = 28.00$, $P < 0.001$) mutant mice spent significantly less time on the rotating rod than the corresponding $Nkx2\text{-}1^{fl/fl}$ control mice (Fig. 6C).

Postnatal *Nkx2-1* deletion in ChAT-expressing cells caused sex-specific deficits in spatial learning (Berger-Sweeney, 2003). Female $ChAT^{cre/+};Nkx2\text{-}1^{fl/fl}$ [$\chi^2_7=27.22$ ($n = 7$), $P < 0.001$] and control mice learned to locate the platform during the place version [$\chi^2_7=28.43$ ($n = 7$), $P < 0.001$]. However, direct comparison of the two performances using Mann–Whitney rank sum-tests revealed that on days 6 and 8 female mutant mice needed significantly more time to locate the platform (Fig. 6E, left). The slightly impaired performance of female mutant mice in the place version was reflected by the spatial probe. These animals showed no significant difference in the time spent in the platform quadrant compared with the mean of the three remaining quadrants ($P = 0.098$; Fig. 6F). In contrast, female control mice spent significantly more time in the former platform quadrant ($P = 0.016$). This impairment of the female mutant mice is not related to visual-motor deficits as they showed a comparable performance to female control mice in the cued version (Fig. 6E). It should be noted here that female mutant mice display longer swimming paths (Fig. 6H) at higher swim speed than female control mice (data not shown).

Both mutant [$\chi^2_7=38.67$ ($n = 7$), $P < 0.001$] and control [$\chi^2_7=36.29$ ($n = 7$), $P < 0.001$] male mice showed good performances in the place version of the MWM (Fig. 6E, right). This was also reflected by the spatial probe, in which mice of both genotypes remembered the former location of the platform (Fig. 6F). There were also no differences in the cued version of the MWM (see Fig. 6E, right).

Finally, the rota-rod test showed no motor deficit for female ($t_6 = 39.00$, $P = 0.491$) and male ($t_6 = 49.00$, $P = 0.463$) *ChAT*$^{cre/+}$;*Nkx2-1*$^{fl/fl}$ mice and their corresponding control mice (Fig. 6G).

Expression of NKX2-1 in the human basal ganglia

As mentioned in the Introduction, human haploinsufficiency for NKX2-1 is accompanied by severe impairments of coordinated movements. Consistently, we have recently shown that Nkx2-1 expression is maintained throughout life by many cholinergic and GABAergic neurons of the mouse ventral forebrain, including the CPu and LGP (Magno *et al.*, 2009). To determine whether NKX2-1 is also expressed by the same neurons in humans, we analysed tissue samples obtained from the basal ganglia. Overall, IHC for NKX2-1 resulted in a more intense darkening of the external part of the globus pallidus (GPe) compared with its internal part (GPi; Fig. 7A). Accordingly, many more NKX2-1-immunoreactive cell profiles could be detected in the GPe (inset in Fig. 7A). Double-IF showed that most NKX2-1-positive cells expressed NeuN and GAD67 (Fig. 7B–G). A smaller proportion of these cells co-expressed PV (in the GPe; Fig. 7H–J) or ChAT (Fig. 7K–M).

Discussion

A recent study has shown that a certain degree of gene expression established at prenatal stages is maintained into adulthood. It was suggested that this embryonic ‘imprint’ could be important for the maintenance of the phenotype and connectivity of already established neuronal populations (Zapala *et al.*, 2005). It is well described (see Introduction) that expression of the transcription factor Nkx2-1 is of fundamental importance for the specification of several neuronal populations. Here we investigated whether prenatal and postnatal expression of the transcription factor is necessary for the integrity of the cholinergic neurons of the basal forebrain.

Targeting of Nkx2-1 in GAD67- and ChAT-expressing cells in the ventral telencephalon

Nkx2-1 becomes detectable around E9 in the neuroepithelium of ventro-medial parts of the telencephalic vesicle, which subsequently differentiates into the medial ganglionic eminence and the preoptic area (Sussel *et al.*, 1999; Puelles *et al.*, 2000). Notably, transcripts for *GAD67* have also been found as early as E10 in the differentiating zones of these regions (Katarova *et al.*, 2000). Several reports (Sussel *et al.*, 1999; Marin *et al.*, 2000; Magno *et al.*, 2009; Nobrega-Pereira *et al.*, 2010), including a recent fate-mapping study (Xu *et al.*, 2008), have shown that Nkx2-1-lineage cells of the subpallium mostly differentiate into cholinergic and GABAergic neurons. Thus, the nearly complete loss of cholinergic and PV-positive neurons observed after early inactivation of the *Nkx2-1* gene in *GAD*$^{cre/+}$;*Nkx2-1*$^{fl/fl}$ mice corresponds to the findings of these earlier studies. In contrast, precursors of cortical GABAergic interneurons (Butt *et al.*, 2005, 2008), which rapidly downregulate *Nkx2-1* expression prior to their migration to the cortical mantle (Nobrega-Pereira *et al.*, 2008), were most likely not affected, as the number of cortical cholinergic or PV-positive GABAergic interneurons, including synthesis of NGF by the latter (present study; cf. Rocamora *et al.*, 1996; McAllister *et al.*, 1999), appeared unchanged. Similarly, no obvious cell loss was observed for striatal SOM-expressing GABAergic neurons, which are also known to downregulate the expression of Nkx2-1 as they exit the neuroepithelium (Marin *et al.*, 2000). As Nkx2-1 protein and mRNA was not detectable in the differentiating nuclei of the ventral telencephalon of *GAD*$^{cre/+}$;*Nkx2-1*$^{fl/fl}$ mice prior to birth, the persistence of a small number of neurons immunoreactive for ChAT or PV in the regions studied could be explained by their origin in Nkx2-1-negative domains (Flames *et al.*, 2007; Garcia-Lopez *et al.*, 2008).

To determine a possible postnatal role of the transcription factor, we targeted *Nkx2-1* in ChAT-expressing cells. Several studies performed in rodents have shown that ChAT synthesis reaches mature levels around P15 (Korsching, 1993; Bender *et al.*, 1996; Naumann *et al.*, 2002). In line with this, ChAT-driven Cre activity was first observed between P4 and P6 (present study). This observation probably explains why targeting of *Nkx2-1* in $ChAT^{cre/+};Nkx2\text{-}1^{fl/fl}$ mice had no effect on the number of ChAT-ir neurons until P15.

The fate of Nkx2-1-deficient cholinergic and PV-expressing GABAergic neurons

Recent studies have revealed that Nkx2-1 plays an important role in the cell-type specification by suppressing the cell fate programmes of the surrounding caudal and lateral ganglionic eminences (Sussel *et al.*, 1999; Butt *et al.*, 2008). Thus, it would be conceivable that the effects of prenatal *Nkx2-1* ablation resulted in enhanced generation of other, non-Nkx2-1-dependent neurons. Moreover, Nkx2-1 ablation could lead to migration of such cells to different target regions (Nobrega-Pereira *et al.*, 2008). However, the results of our fine-structural analysis do not support these possibilities. The presence of cells in the MGE showing severe signs of degeneration leads to the conclusion that prenatal deletion of Nkx2-1 causes substantial local cell loss rather than changes in cell fate and/or migratory behaviour. Accordingly, the LGP, known to contain a very high number of neurons expressing Nkx2-1 at postnatal stages, is much smaller in $GAD\text{-}^{cre/+};Nkx2\text{-}1^{fl/fl}$ mice due to a strong reduction of the total cell number. This also shows that prenatal deletion of *Nkx2-1* is unlikely to cause the generation of functionally different neurons for this heavily affected region (cf. Butt *et al.*, 2008).

Proper development of the forebrain nuclei depends on the expression of several transcription factors (Sussel *et al.*, 1999; Marin *et al.*, 2000; Fragkouli *et al.*, 2005; Flandin *et al.*, 2010; Nobrega-Pereira *et al.*, 2010). Nkx2-1 has been shown to regulate the expression of downstream targets such as members of the LIM home domain family, Lhx6 and Lhx7 (Sussel *et al.*, 1999; Fragkouli *et al.*, 2005). Additional analysis of the expression pattern of Lhx6 and Lhx7 transcripts further confirmed that cholinergic and PV-positive neurons were almost completely absent in the four regions investigated. These data are also in line with the nearly complete lack of cholinergic fibres in the target structures of the cholinergic basal forebrain neurons. Finally, the lack of fine-structural hallmarks of ongoing degeneration in young adult and adult $GAD^{cre/+};Nkx2\text{-}1^{fl/fl}$ animals (e.g. long-lasting activation of microglia, cell debris; cf. Hollerbach *et al.*, 1998) supports the idea that the affected neurons died rapidly and were removed locally within a very short time.

In contrast, the loss of cholinergic neurons in the $ChAT^{cre/+};Nkx2\text{-}1^{fl/fl}$ mice is probably a result of prolonged degeneration. As was seen for septal neurons following axotomy or excitotoxic lesions performed in early postnatal and adult rodents (cf. Naumann *et al.*, 1992b; Plaschke *et al.*, 1997), numerous cells exhibited a very electron-dense cytoplasm, and intact organelles or membranes could barely be detected. The presence of such cell profiles was most frequently observed in tissue probes obtained from 4- to 8-week-old mutant mice. It should also be mentioned here that additional IHC for detection of apoptotic cell death (e.g. by using antibodies against caspase 3) never resulted in substantial labelling of cells in the various subcortical nuclei. Moreover, in $ChAT^{cre/+};Nkx2\text{-}1^{fl/fl}$ mice degenerating neurons were observed in close proximity to intact ChAT-ir neurons (cf. Naumann *et al.*, 1992a). This indicates the heterogeneity of cholinergic basal forebrain neurons. As shown from cell counts at 6 months of age, as well as the results gained from our crossings of the mutants with the ROSA26LacZ indicator strain, the remaining large set of cholinergic neurons is not affected by the mutation because they have most likely down-regulated Nkx2-1 synthesis prior to upregulation of ChAT and Cre. A third, and very small, subset of these neurons could derive from Nkx2-1-negative domains (see above) and is, with the methods applied, indistinguishable from the former population. In line with this, the

decrease in the expression levels of the NGF-receptors trkA and $p75^{NTR}$ (for reviews see Chao & Hempstead, 1995; Thoenen, 1995) and the loss of cholinergic fibres in the target structures of the cholinergic neurons were found to be attenuated in *ChAT*$^{cre/+}$;*Nkx2-1*$^{fl/fl}$ mice compared with those of *GAD*$^{cre/+}$;*Nkx2-1*$^{fl/fl}$ mice.

Functional implications for pre- and postnatal mutations of Nkx2-1 transcription factor

In Nkx2-1 knockout mice, a substantial loss of cortical interneurons was observed together with severe morphological alterations of the basal ganglia and various nuclei of the diencephalon (Kimura *et al.*, 1996). Recently, it was shown that a postnatal synapsin I-driven deletion of the *Nkx2-1* gene led to various vegetative dysfunctions (for reviews see Son *et al.*, 2003; Kim *et al.*, 2006) due to alterations restricted to the hypothalamus (Mastronardi *et al.*, 2006). On the other hand, humans suffering from NKX2-1-haploinsufficiency show severe deficit of coordinated movement, but notable impairments of higher cognitive functions or those related to the function of the diencephalon have not yet been described (reviewed by Kleiner-Fisman & Lang, 2007). In the present study, we show that *GAD*$^{cre/+}$;*Nkx2-1*$^{fl/fl}$ mice have lost nearly all striatal cholinergic and PV-positive interneurons. In addition, a severe loss of the projection neurons in the LGP targeting the subthalamic nucleus or the substantia nigra (reviewed by Gerfen, 2004) was observed. Thus, the pronounced impairment of coordinated movement in these animals points to severe deficits within the loops of the motorcortex–CPu–LGP axis. Although the prenatal Nkx2-1 mutation in mice cannot be directly considered as a model for the human NKX2-1 haploinsufficiency, the neurological symptoms of the patients can be partially explained by the results obtained from these mice. In fact, expression of the transcription factor by cholinergic and PV-positive neurons was detected in the telencephalic parts of the basal ganglia of humans (present study) and mice (Magno *et al.*, 2009). Little is known about the function of these neuronal subpopulations (e.g. Calabresi *et al.*, 2000) although in *ChAT*$^{cre/+}$;*Nkx2-1*$^{fl/fl}$ mice the remaining cholinergic interneurons are obviously sufficient to compensate for the cell loss, at least until 3 months of age.

In our experiments, the almost complete loss of cholinergic neurons in *GAD*$^{cre/+}$;*Nkx2-1*$^{fl/fl}$ mice resulted in severe impairments of learning and spatial memory functions. This correlates with the results of many excellent studies that have highlighted the central role of the cholinergic ventral forebrain systems projecting to nearly all parts of the telencephalon, including the neocortical mantle, the hippocampal formation and the amygdaloid complex (Berger-Sweeney, 2003; McKinney & Jacksonville, 2005). However, our results are only partially comparable with those obtained by other prenatal mutations of the cholinergic basal forebrain system, e.g. following deletion of *Lhx7*. Although *Lhx7* mutation has also been described as causing disturbances in spatial learning and memory, Lhx7-deficient mice displayed normal locomotor activity and motor coordination (Fragkouli *et al.*, 2005, 2009a). This discrepancy could be explained by the fact that we have targeted PV-positive GABAergic neurons in addition to their cholinergic counterparts. In fact, GABAergic neurons of the ventral forebrain contribute significantly to the long projections that originate in the large magnocellular nuclei (Freund, 1989; Kermer *et al.*, 1995; Gritti *et al.*, 1997). It remains unclear to what extent the loss of GABAergic neurons might have contributed to the deficits in higher cognitive functions, as their role has been less intensively investigated than that of the cholinergic neurons (Schwegler *et al.*, 1996). However, previous studies have also shown that deficits in higher cognitive functions, resulting from manipulation of the cholinergic systems, are less pronounced if performed in adult rodents (Berger-Sweeney, 2003). Indeed, in our study only a minor deficit in spatial learning and memory was observed for female *ChAT*$^{cre/+}$; *Nkx2-1*$^{fl/fl}$ mice (cf. Arters *et al.*, 1998; Berger-Sweeney, 2003; Fragkouli *et al.*, 2009a). A more detailed analysis performed for the MSvDB and hDB-SI did not provide evidence for a sex-specific effect of the mutations, at least at the

level of cell numbers. It is reasonable to assume that more subtle changes contribute to cognitive impairments because prenatal targeting of Nkx2-1 expression was also found to be accompanied by an aberrant development of axonal projections in several regions of the mouse brain (Kawano *et al.*, 2003).

Our study shows that (i) prenatal expression of Nkx2-1 is a prerequisite for the development of cholinergic neurons of the ventral forebrain and (ii) postnatal targeting of this transcription factor is still accompanied by substantial neuronal degeneration, corresponding target denervation, and mild impairments of the spatial memory.

Acknowledgments

We would like to thank H. Schwegler, H-D. Hofmann and J. A. Liebkowsky for critical reading of our manuscript. We also would like to thank G. Thomaschek, C. Guijarro, A. Steuer, J. Schuler and A. Wistel-Wozniak for their technical assistance. This work was supported by the DFG, Sonderforschungsbereich 665/A3 (Berlin) until 2009, and thereafter by B3.

Abbreviations

AChE	acetylcholine esterase
CB	calbindin
ChAT	choline acetyltransferase
CPu	caudate putamen
CR	calretinin
GAD67	glutamate decarboxylase 67
GPe	globus pallidus - external segment
GPi	globus pallidus - internal segment
hDB-SI	horizontal limb of the diagonal band-substantia innominata
IHC	immunohistochemistry
ir	immunoreactive
ISH	*in situ* hybridization
LGP	lateral globus pallidus
LS	lateral septum
MGE	medial ganglionic eminence
MS	medial septum
MSvDB	medial septum-ventral limb of the diagonal band
MWM	Morris water maze
PB	phosphate buffer
PFA	paraformaldehyde
POA	preoptic area
PV	parvalbumin
SOM	somatostatin
SVZ	subventricular zone

VZ ventricular zone

References

Arters J, Hohmann CF, Mills J, Olaghere O, Berger-Sweeney J. Sexually dimorphic responses to neonatal basal forebrain lesions in mice: I. Behavior and neurochemistry. J Neurobiol. 1998; 37:582–594. [PubMed: 9858260]

Bayer SA. The development of the septal region in the rat. I Neurogenesis examined with 3H-thymidine autoradiography. J Comp Neurol. 1979; 183:89–106. [PubMed: 758337]

Bender R, Plaschke M, Naumann T, Wahle P, Frotscher M. Development of cholinergic and GABAergic neurons in the rat medial septum: different onset of choline acetyltransferase and glutamate decarboxylase mRNA expression. J Comp Neurol. 1996; 372:204–214. [PubMed: 8863126]

Berger-Sweeney J. The cholinergic basal forebrain system during development and its influence on cognitive processes: important questions and potential answers. Neurosci Biobehav Rev. 2003; 27:401–411. [PubMed: 12946692]

Bert B, Fink H, Huston JP, Voits M. Fischer 344 and wistar rats differ in anxiety and habituation but not in water maze performance. Neurobiol Learn Mem. 2002; 78:11–22. [PubMed: 12071664]

Bert B, Dere E, Wilhelmi N, Kusserow H, Theuring F, Huston JP, Fink H. Transient overexpression of the 5-HT1A receptor impairs water-maze but not hole-board performance. Neurobiol Learn Mem. 2005; 84:57–68. [PubMed: 15936683]

Bibel M, Barde YA. Neurotrophins: key regulators of cell fate and cell shape in the vertebrate nervous system. Genes Dev. 2000; 14:2919–2937. [PubMed: 11114882]

Bonsi P, Cuomo D, Martella G, Madeo G, Schirinzi T, Puglisi F, Ponterio G, Pisani A. Centrality of striatal cholinergic transmission in Basal Ganglia function. Front Neuroanat. 2011; 5:6. [PubMed: 21344017]

Breedveld GJ, van Dongen JW, Danesino C, Guala A, Percy AK, Dure LS, Harper P, Lazarou LP, van der Linde H, Joosse M, Gruters A, MacDonald ME, de Vries BB, Arts WF, Oostra BA, Krude H, Heutink P. Mutations in TITF-1 are associated with benign hereditary chorea. Hum Mol Genet. 2002; 11:971–979. [PubMed: 11971878]

Buhl EH, Schlote W. Intracellular lucifer yellow staining and electron microscopy of neurones in slices of fixed epitumourous human cortical tissue. Acta Neuropathol. 1987; 75:140–146. [PubMed: 3434221]

Butt SJ, Fuccillo M, Nery S, Noctor S, Kriegstein A, Corbin JG, Fishell G. The temporal and spatial origins of cortical interneurons predict their physiological subtype. Neuron. 2005; 48:591–604. [PubMed: 16301176]

Butt SJ, Sousa VH, Fuccillo MV, Hjerling-Leffler J, Miyoshi G, Kimura S, Fishell G. The requirement of Nkx2-1 in the temporal specification of cortical interneuron subtypes. Neuron. 2008; 59:722–732. [PubMed: 18786356]

Calabresi P, Centonze D, Gubellini P, Pisani A, Bernardi G. Acetylcholine-mediated modulation of striatal function. Trends Neurosci. 2000; 23:120–126. [PubMed: 10675916]

do Carmo Costa M, Costa C, Silva AP, Evangelista P, Santos L, Ferro A, Sequeiros J, Maciel P. Nonsense mutation in TITF1 in a Portuguese family with benign hereditary chorea. Neurogenetics. 2005; 6:209–215. [PubMed: 16220345]

Chao MV, Hempstead BL. p75 and Trk: a two-receptor system. Trends Neurosci. 1995; 18:321–326. [PubMed: 7571013]

Du T, Xu Q, Ocbina PJ, Anderson SA. NKX2.1 specifies cortical interneuron fate by activating Lhx6. Development. 2008; 135:1559–1567. [PubMed: 18339674]

Eckenstein F, Sofroniew MV. Identification of central cholinergic neurons containing both choline acetyltransferase and acetylcholinesterase and of central neurons containing only acetylcholinesterase. J Neurosci. 1983; 3:2286–2291. [PubMed: 6355402]

Flames N, Pla R, Gelman DM, Rubenstein JL, Puelles L, Marin O. Delineation of multiple subpallial progenitor domains by the combinatorial expression of transcriptional codes. J Neurosci. 2007; 27:9682–9695. [PubMed: 17804629]

Flandin P, Kimura S, Rubenstein JL. The progenitor zone of the ventral medial ganglionic eminence requires Nkx2-1 to generate most of the globus pallidus but few neocortical interneurons. J Neurosci. 2010; 30:2812–2823. [PubMed: 20181579]

Fragkouli A, Hearn C, Errington M, Cooke S, Grigoriou M, Bliss T, Stylianopoulou F, Pachnis V. Loss of forebrain cholinergic neurons and impairment in spatial learning and memory in LHX7-deficient mice. Eur J Neurosci. 2005; 21:2923–2938. [PubMed: 15978004]

Fragkouli A, Pachnis V, Stylianopoulou F. Sex differences in water maze performance and cortical neurotrophin levels of LHX7 null mutant mice. Neuroscience. 2009a; 158:1224–1233. [PubMed: 19095044]

Fragkouli A, van Wijk NV, Lopes R, Kessaris N, Pachnis V. LIM homeodomain transcription factor-dependent specification of bipotential MGE progenitors into cholinergic and GABAergic striatal interneurons. Development. 2009b; 136:3841–3851. [PubMed: 19855026]

Freund TF. GABAergic septohippocampal neurons contain parvalbumin. Brain Res. 1989; 478:375–381. [PubMed: 2924136]

Garcia-Lopez M, Abellan A, Legaz I, Rubenstein JL, Puelles L, Medina L. Histogenetic compartments of the mouse centromedial and extended amygdala based on gene expression patterns during development. J Comp Neurol. 2008; 506:46–74. [PubMed: 17990271]

Gerfen, CR. Basal ganglia. In: Paxinos, G., editor. The Rat Nervous System. Elsevier Academic Press; San Diego: 2004. p. 455-509.

Gnahn H, Hefti F, Heumann R, Schwab ME, Thoenen H. NGF-mediated increase of choline acetyltransferase (ChAT) in the neonatal rat forebrain: evidence for a physiological role of NGF in the brain? Brain Res. 1983; 285:45–52. [PubMed: 6136314]

Gritti I, Mainville L, Mancia M, Jones BE. GABAergic and other noncholinergic basal forebrain neurons, together with cholinergic neurons, project to the mesocortex and isocortex in the rat. J Comp Neurol. 1997; 383:163–177. [PubMed: 9182846]

Hollerbach EH, Haas CA, Hildebrandt H, Frotscher M, Naumann T. Region-specific activation of microglial cells in the rat septal complex following fimbria-fornix transection. J Comp Neurol. 1998; 390:481–496. [PubMed: 9450531]

Katarova Z, Sekerkova G, Prodan S, Mugnaini E, Szabo G. Domain-restricted expression of two glutamic acid decarboxylase genes in midgestation mouse embryos. J Comp Neurol. 2000; 424:607–627. [PubMed: 10931484]

Kawano H, Horie M, Honma S, Kawamura K, Takeuchi K, Kimura S. Aberrant trajectory of ascending dopaminergic pathway in mice lacking Nkx2.1. Exp Neurol. 2003; 182:103–112. [PubMed: 12821380]

Kermer P, Naumann T, Bender R, Frotscher M. Fate of GABAergic septohippocampal neurons after fimbria-fornix transection as revealed by in situ hybridization for glutamate decarboxylase mRNA and parvalbumin immunocytochemistry. J Comp Neurol. 1995; 362:385–399. [PubMed: 8576446]

Kim JG, Nam-Goong IS, Yun CH, Jeong JK, Kim ES, Park JJ, Lee YC, Kim YI, Lee BJ. TTF-1, a homeodomain-containing transcription factor, regulates feeding behavior in the rat hypothalamus. Biochem Biophys Res Commun. 2006; 349:969–975. [PubMed: 16970909]

Kimura S, Hara Y, Pineau T, Fernandez-Salguero P, Fox CH, Ward JM, Gonzalez FJ. The T/ebp null mouse: thyroid-specific enhancer-binding protein is essential for the organogenesis of the thyroid, lung, ventral forebrain, and pituitary. Genes Dev. 1996; 10:60–69. [PubMed: 8557195]

Kleiner-Fisman G, Lang AE. Benign hereditary chorea revisited: a journey to understanding. Mov Disord. 2007; 22:2297–2305. quiz 2452. [PubMed: 17702033]

Korsching S. The neurotrophic factor concept: a reexamination. J Neurosci. 1993; 13:2739–2748. [PubMed: 8331370]

Krude H, Schutz B, Biebermann H, von Moers A, Schnabel D, Neitzel H, Tonnies H, Weise D, Lafferty A, Schwarz S, DeFelice M, von Deimling A, van Landeghem F, DiLauro R, Gruters A. Choreoathetosis, hypothyroidism, and pulmonary alterations due to human NKX2-1 haploinsufficiency. J Clin Invest. 2002; 109:475–480. [PubMed: 11854319]

Kusakabe T, Kawaguchi A, Hoshi N, Kawaguchi R, Hoshi S, Kimura S. Thyroid-specific enhancer-binding protein/NKX2.1 is required for the maintenance of ordered architecture and function of the differentiated thyroid. Mol Endocrinol. 2006; 20:1796–1809. [PubMed: 16601074]

Li Y, Holtzman DM, Kromer LF, Kaplan DR, Chua-Couzens J, Clary DO, Knusel B, Mobley WC. Regulation of TrkA and ChAT expression in developing rat basal forebrain: evidence that both exogenous and endogenous NGF regulate differentiation of cholinergic neurons. J Neurosci. 1995; 15:2888–2905. [PubMed: 7536822]

Magno L, Catanzariti V, Nitsch R, Krude H, Naumann T. Ongoing expression of Nkx2.1 in the postnatal mouse forebrain: potential for understanding NKX2.1 haploinsufficiency in humans? Brain Res. 2009; 1304:164–186. [PubMed: 19766601]

Marin O, Anderson SA, Rubenstein JL. Origin and molecular specification of striatal interneurons. J Neurosci. 2000; 20:6063–6076. [PubMed: 10934256]

Mastronardi C, Smiley GG, Raber J, Kusakabe T, Kawaguchi A, Matagne V, Dietzel A, Heger S, Mungenast AE, Cabrera R, Kimura S, Ojeda SR. Deletion of the Ttf1 gene in differentiated neurons disrupts female reproduction without impairing basal ganglia function. J Neurosci. 2006; 26:13167–13179. [PubMed: 17182767]

McAllister AK, Katz LC, Lo DC. Neurotrophins and synaptic plasticity. Annu Rev Neurosci. 1999; 22:295–318. [PubMed: 10202541]

McKinney M, Jacksonville MC. Brain cholinergic vulnerability: relevance to behavior and disease. Biochem Pharmacol. 2005; 70:1115–1124. [PubMed: 15975560]

Mesulam MM, Mufson EJ, Levey AI, Wainer BH. Cholinergic innervation of cortex by the basal forebrain: cytochemistry and cortical connections of the septal area, diagonal band nuclei, nucleus basalis (substantia innominata), and hypothalamus in the rhesus monkey. J Comp Neurol. 1983; 214:170–197. [PubMed: 6841683]

Mizuno K, Carnahan J, Nawa H. Brain-derived neurotrophic factor promotes differentiation of striatal GABAergic neurons. Dev Biol. 1994; 165:243–256. [PubMed: 8088442]

Mobley WC, Rutkowski JL, Tennekoon GI, Gemski J, Buchanan K, Johnston MV. Nerve growth factor increases choline acetyltransferase activity in developing basal forebrain neurons. Brain Res. 1986; 387:53–62. [PubMed: 3742234]

Naumann T, Linke R, Frotscher M. Fine structure of rat septohippocampal neurons: I. Identification of septohippocampal projection neurons by retrograde tracing combined with electron microscopic immunocytochemistry and intracellular staining. J Comp Neurol. 1992a; 325:207–218. [PubMed: 1281173]

Naumann T, Peterson GM, Frotscher M. Fine structure of rat septohippocampal neurons: II. A time course analysis following axotomy. J Comp Neurol. 1992b; 325:219–242. [PubMed: 1460114]

Naumann T, Casademunt E, Hollerbach E, Hofmann J, Dechant G, Frotscher M, Barde YA. Complete deletion of the neurotrophin receptor p75NTR leads to long-lasting increases in the number of basal forebrain cholinergic neurons. J Neurosci. 2002; 22:2409–2418. [PubMed: 11923404]

Nobrega-Pereira S, Kessaris N, Du T, Kimura S, Anderson SA, Marin O. Postmitotic Nkx2-1 controls the migration of telencephalic interneurons by direct repression of guidance receptors. Neuron. 2008; 59:733–745. [PubMed: 18786357]

Nobrega-Pereira S, Gelman D, Bartolini G, Pla R, Pierani A, Marin O. Origin and molecular specification of globus pallidus neurons. J Neurosci. 2010; 30:2824–2834. [PubMed: 20181580]

Paxinos, GFK. The Mouse Brain in Stereotaxic Coordinates. Academic Press; San Diego: 2001.

Plaschke M, Naumann T, Kasper E, Bender R, Frotscher M. Development of cholinergic and GABAergic neurons in the rat medial septum: effect of target removal in early postnatal development. J Comp Neurol. 1997; 379:467–481. [PubMed: 9067837]

Pohlenz J, Dumitrescu A, Zundel D, Martine U, Schonberger W, Koo E, Weiss RE, Cohen RN, Kimura S, Refetoff S. Partial deficiency of thyroid transcription factor 1 produces predominantly neurological defects in humans and mice. J Clin Invest. 2002; 109:469–473. [PubMed: 11854318]

Puelles L, Kuwana E, Puelles E, Bulfone A, Shimamura K, Keleher J, Smiga S, Rubenstein JL. Pallial and subpallial derivatives in the embryonic chick and mouse telencephalon, traced by the expression of the genes Dlx-2, Emx-1, Nkx-2.1, Pax-6, and Tbr-1. J Comp Neurol. 2000; 424:409–438. [PubMed: 10906711]

Reichardt LF. Neurotrophin-regulated signalling pathways. Philos Trans R Soc Lond B Biol Sci. 2006; 361:1545–1564. [PubMed: 16939974]

Rocamora N, Pascual M, Acsady L, de Lecea L, Freund TF, Soriano E. Expression of NGF and NT3 mRNAs in hippocampal interneurons innervated by the GABAergic septohippocampal pathway. J Neurosci. 1996; 16:3991–4004. [PubMed: 8656293]

Schuurmans C, Guillemot F. Molecular mechanisms underlying cell fate specification in the developing telencephalon. Curr Opin Neurobiol. 2002; 12:26–34. [PubMed: 11861161]

Schwegler H, Boldyreva M, Linke R, Wu J, Zilles K, Crusio WE. Genetic variation in the morphology of the septo-hippocampal cholinergic and GABAergic systems in mice: II. Morpho-behavioral correlations. Hippocampus. 1996; 6:535–545. [PubMed: 8953306]

Sobreviela T, Clary DO, Reichardt LF, Brandabur MM, Kordower JH, Mufson EJ. TrkA-immunoreactive profiles in the central nervous system: colocalization with neurons containing p75 nerve growth factor receptor, choline acetyltransferase, and serotonin. J Comp Neurol. 1994; 350:587–611. [PubMed: 7890832]

Sofroniew MV, Pearson RC, Powell TP. The cholinergic nuclei of the basal forebrain of the rat: normal structure, development and experimentally induced degeneration. Brain Res. 1987; 411:310–331. [PubMed: 3607436]

Sofroniew MV, Howe CL, Mobley WC. Nerve growth factor signaling, neuroprotection, and neural repair. Annu Rev Neurosci. 2001; 24:1217–1281. [PubMed: 11520933]

Son YJ, Hur MK, Ryu BJ, Park SK, Damante G, D'Elia AV, Costa ME, Ojeda SR, Lee BJ. TTF-1, a homeodomain-containing transcription factor, participates in the control of body fluid homeostasis by regulating angiotensinogen gene transcription in the rat subfornical organ. J Biol Chem. 2003; 278:27043–27052. [PubMed: 12730191]

Sussel L, Marin O, Kimura S, Rubenstein JL. Loss of Nkx2.1 homeobox gene function results in a ventral to dorsal molecular respecification within the basal telencephalon: evidence for a transformation of the pallidum into the striatum. Development. 1999; 126:3359–3370. [PubMed: 10393115]

Thoenen H. Neurotrophins and neuronal plasticity. Science. 1995; 270:593–598. [PubMed: 7570017]

West MJ, Slomianka L, Gundersen HJ. Unbiased stereological estimation of the total number of neurons in thesubdivisions of the rat hippocampus using the optical fractionator. Anat Rec. 1991; 231:482–497. [PubMed: 1793176]

Wigle JT, Eisenstat DD. Homeobox genes in vertebrate forebrain development and disease. Clin Genet. 2008; 73:212–226. [PubMed: 18241223]

Xu Q, Tam M, Anderson SA. Fate mapping Nkx2.1-lineage cells in the mouse telencephalon. J Comp Neurol. 2008; 506:16–29. [PubMed: 17990269]

Yoon SO, Casaccia-Bonnefil P, Carter B, Chao MV. Competitive signaling between TrkA and p75 nerve growth factor receptors determines cell survival. J Neurosci. 1998; 18:3273–3281. [PubMed: 9547236]

Zapala MA, Hovatta I, Ellison JA, Wodicka L, Del Rio JA, Tennant R, Tynan W, Broide RS, Helton R, Stoveken BS, Winrow C, Lockhart DJ, Reilly JF, Young WG, Bloom FE, Barlow C. Adult mouse brain gene expression patterns bear an embryologic imprint. Proc Natl Acad Sci USA. 2005; 102:10357–10362. [PubMed: 16002470]

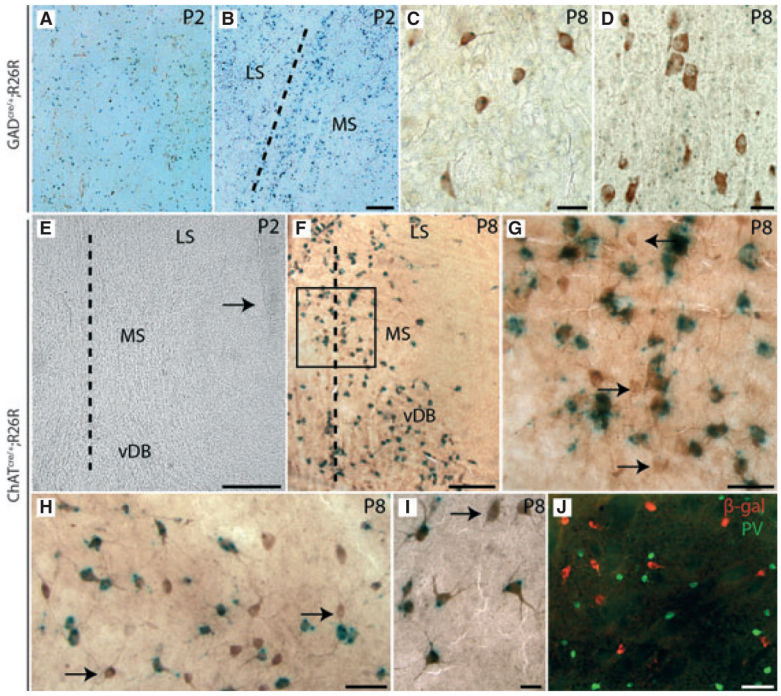

Fig. 1.

Cre-recombination in the subcortical telencephalon of *GAD*$^{cre/+}$*;R26R* and *ChAT*$^{cre/+}$*;R26R* mice. (A–D) X-gal staining is shown for *GAD*$^{cre/+}$*;R26R* mice at P2 (A, B) and P8 (C, D). As shown here by representative coronal sections, an intense punctuate-like labelling was observed in newborn animals throughout the telencephalon including the CPu (A) and within the septal complex (B). The border between the medial septum (MS) and the lateral septal complex (LS) is marked by a dotted line (B). From P7–8 onwards, these precipitates could be localized in GABAergic and cholinergic neurons. As shown here for the CPu (C) and the MS (D), nearly all of the ChAT-ir neurons of the ventral forebrain were also found to be positive for X-gal. Scale bars – 50 μm (A, B), 30 μm (C), 20 μm (D). (E–J) In *ChAT*$^{cre/+}$*;R26R* mice, no labelling for X-gal was observed prior to or shortly after birth in the telencephalon. A corresponding coronal section obtained at P2 is shown (E). The ventricle located lateral to the various septal nuclei (MS, vDB, LS) is marked by an arrow. The dotted lines (E, F) indicate the median axis of the brain. (F–J) At P8, intense green punctuate-like labelling for X-gal was observed in all cholinergic centres of the ventral forebrain including the MSvDB (F; boxed area is shown at higher magnification in G), the magnocellular complex of the hDB-SI (H), and in the CPu (I). In these regions, the overwhelming majority of X-gal-positive cells could be identified as cholinergic neurons following subsequent IHC for ChAT (brown labelling of cells; F–I). Only a small subset of ChAT-ir neurons did not present any labelling for X-gal (marked by arrows in G–I). In *ChAT*$^{cre/+}$*;R26R* mice, activity of Cre recombinase was found to be restricted to cholinergic neurons. As shown for the CPu, no co-localization of the two markers β-gal (red cells) and PV (green cells) could be detected in the ventral forebrain (J). Scale bars –100 μm (E, J), 200 μm (F), 50 μm (G, H) and 10 μm (I).

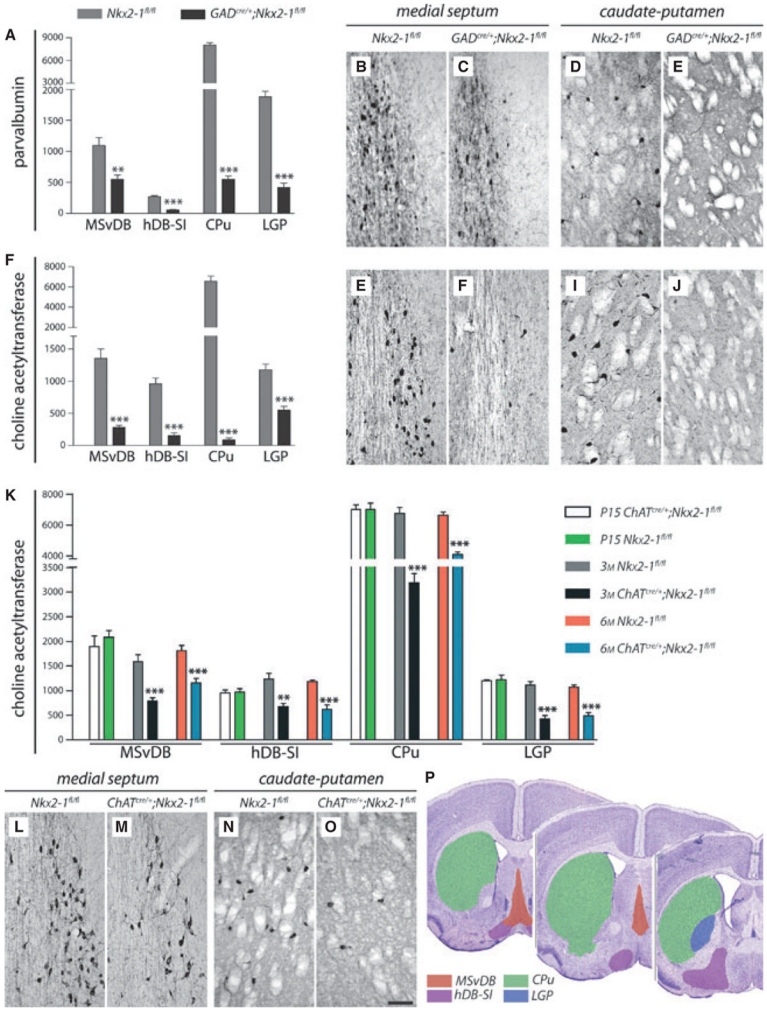

Fig. 2.

Ablation of *Nkx2-1* leads to loss of ChAT- and PV-immunoreactive neurons in the subcortical telencephalon. (A) Stereological cell counts for PV-ir cells of $GAD^{cre/+};Nkx2\text{-}1^{fl/fl}$ mice and $Nkx2\text{-}1^{fl/fl}$ controls (3 months of age) in the four regions investigated are shown. Histograms (see also F and K) show mean (+SEM) cell numbers. Asterisks indicate significant differences – $^{**}P < 0.05$; $^{***}P < 0.001$. (B–E) The loss of PV-ir neurons in $GAD^{cre/+};Nkx2\text{-}1^{fl/fl}$ mice is shown by representative coronal sections for the MSvDB (C) and the CPu (E). In B and D, corresponding sections of $Nkx2\text{-}1^{fl/fl}$ control animals are shown. (F) Stereological cell counts for ChAT-ir cells of $GAD^{cre/+};Nkx2\text{-}1^{fl/fl}$ and $Nkx2\text{-}1^{fl/fl}$ controls (3 months of age) also revealed dramatic cell loss in the four regions investigated. (G–J) The loss of ChAT-ir neurons in $GAD^{cre/+};Nkx2\text{-}1^{fl/fl}$ mutant mice is shown by representative coronal sections of the MSvDB (H) and the CPu (J). For comparison, these regions are also shown for $Nkx2\text{-}1^{fl/fl}$ controls (G, I). (K) Stereological cell counts for ChAT-ir neurons of $ChAT^{cre/+};Nkx2\text{-}1^{fl/fl}$ mice at P15, 3 and 6 months of age of the various regions are shown. Note that at P15 the number of ChAT-ir neurons of the various regions analysed corresponds to the cell number obtained from $Nkx2\text{-}1^{fl/fl}$ controls. Interestingly, no further significant changes in cell number was detected for the control and mutant mice between 3 and 6 months of age. (L–O) The partial loss of ChAT-ir neurons in $ChAT^{cre/+};Nkx2\text{-}1^{fl/fl}$ mice at 3 months of age is shown for the MSvDB (M) and the CPu (O) in comparison with age-matched $Nkx2\text{-}1^{fl/fl}$ controls (L and N). Scale bar (in O) for all

images – 100 μm. (P) The four regions of interest investigated by stereological cell counts are shown at three different levels along the rostro-caudal axis of the mouse brain (modified from Paxinos, 2001). Whereas the borders of the MSvDB, the CPu and the LGP are well described in the literature, no common definition of the so-called 'substantia innominata' yet exists. For practical reasons we used the term 'hDB-SI' because the horizontal part of the diagonal band mainly contributes to this region (see left and middle sections). At more caudal level (right section), neurons of the substantia innominata and the magnocellular preoptic nucleus were also included in the estimations of the total number of cells.

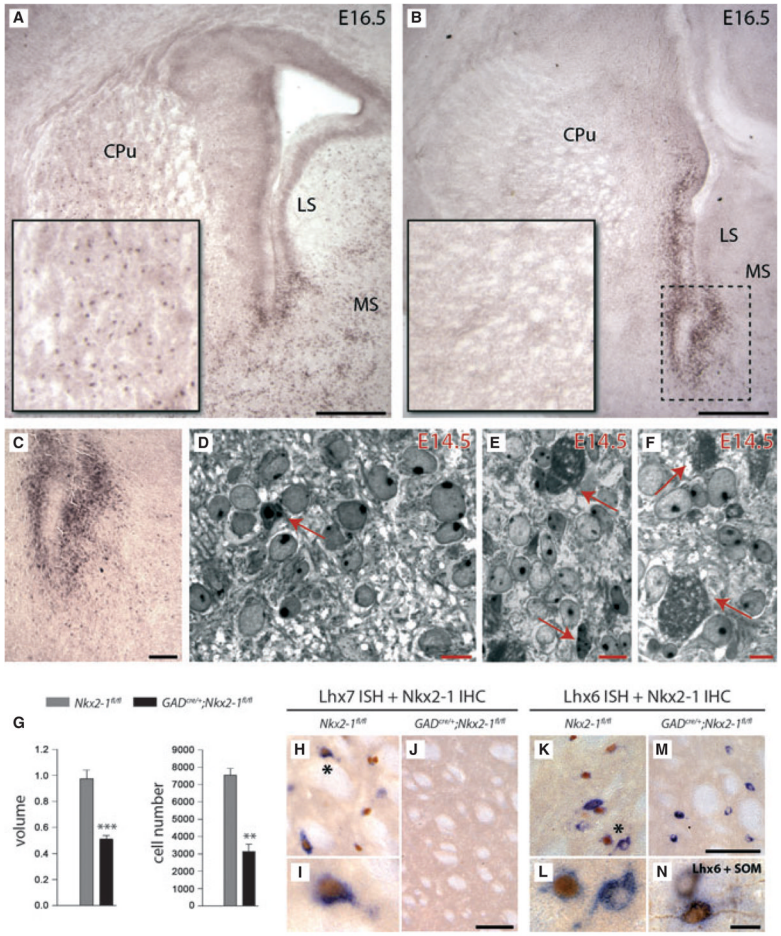

Fig. 3.

Fate of basal forebrain neurons in *GAD*$^{cre/+}$*;Nkx2-1*$^{fl/fl}$ mice. (A, B) IHC for Nkx2-1 for the regions surrounding the lateral ventricle is shown for *Nkx2-1*$^{fl/fl}$ control (A) and mutant *GAD*$^{cre/+}$*;Nkx2-1*$^{fl/fl}$ (B) mice at E16.5. Whereas in control animals intense labelling of cell profiles was predominately observed at the ventral tips of the lateral ventricles (A) and throughout the neighbouring compartments of the subcortical brain including the CPu (A; partially shown at higher magnification in the large inset), the medial septum (MS) and the lateral septum (LS; A), Nkx2-1 immunolabelling was found to be restricted to the ventricular zone in mutant mice (B, dotted frame is shown at higher magnification in C). As shown for the CPu (B, partially shown at higher magnification in the large inset), Nkx2-1-positive cell profiles could barely be detected. Scale bar for A and B – 100 μm, for C – 8 μm. (D–F) Subsequent fine-structural analysis of the subventricular zone of controls (D) and mutant mice (E, F) at E14.5 revealed that in *Nkx2-1*$^{fl/fl}$ mice only occasionally were apoptotic cell profiles observed (D, arrow). In contrast, many cell profiles showing severe signs of degeneration were detectable in mutants at this age (E, F; arrows). Scale bar for D–F – 10 μm. (G) The histograms show the results of the stereological estimations of the total volume (left) and the total number of NeuN-positive cells (right) of the LGP at 3 months of age. The data are presented as volume (mm^3) and cell number + SEM, the bars show average values and significance is indicated by asterisks – $^{**}P < 0.05$; $^{***}P < 0.001$. Both total volume and total number of NeuN-positive cells were significantly reduced in the mutant mice at 3 months of age. (H–N) ISH for *Lhx7* or *Lhx6* combined with IHC for Nkx2-1 (H–M) or SOM (N) are shown for *GAD*$^{cre/+}$*;Nkx2-1*$^{fl/fl}$ and *Nkx2-1*$^{fl/fl}$ at 4 weeks

of age – ISH for Lhx6 and Lhx7 results in violet staining of the cytoplasm (H, I, K–N) while Nkx2-1-ir neurons display brown staining of cell nuclei. One of the neurons double-labelled for Nkx2-1 and *Lhx7* (H, black asterisk) is shown at higher magnification (I). As shown for the CPu at 4 weeks of age, the nearly complete loss of *Lhx7*- and Nkx2-1-expressing cells (J) confirms the dramatic loss of cholinergic neurons in $GAD^{cre/+};Nkx2\text{-}1^{fl/fl}$ mutant mice. However, in these animals, labelling for *Lhx6* was partially maintained (cf. K and M), and most of these cells could be identified as SOM-ir striatal interneurons (N). In the CPu of $Nkx2\text{-}1^{fl/fl}$ mice cells labelled for *Lhx6* and Nkx2-1 are marked by an asterisk in K (shown at higher magnification in L). Scale bars – 100 μm (K, M); 50 μm (C, F and H); 10 μm (D, G and I).

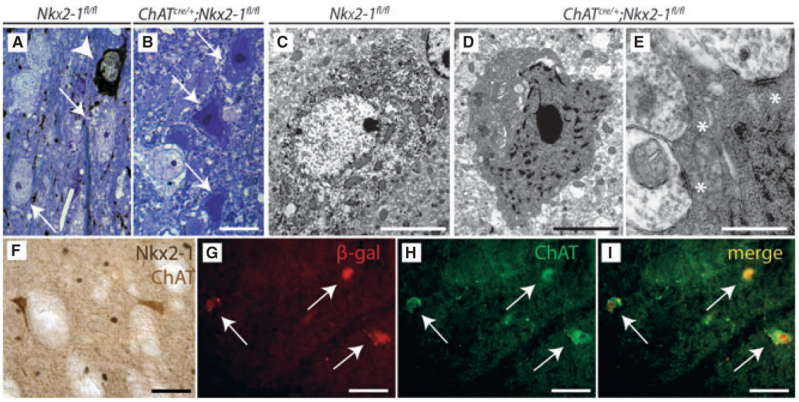

Fig. 4.

Fate of basal forebrain neurons in *ChAT*$^{cre/+}$*;Nkx2-1*$^{fl/fl}$ mice. (A, B) As shown by semithin sections following IHC for ChAT, some cholinergic neurons in *ChAT*$^{cre/+}$*;Nkx2-1*$^{fl/fl}$ mice underwent severe degenerative processes following ablation of *Nkx2-1*. Several unlabelled neurons (A, thin arrows) and one ChAT-ir neuron (A, arrowhead) in the MS of a 4-week-old *Nkx2-1*$^{fl/fl}$ mouse are shown. In the mutant mice, a dramatic increase in the number of dark-coloured neurons (B, arrows) was observed. (C–E) Further fine-structural analysis revealed that many ventral forebrain neurons including those of the MS show signs of severe degenerative changes, including darkening of the cytoplasm and condensation of the chromatin (D, E). Notably, these heavily damaged neurons partially still bore input synapses (E; white asterisks). Similar changes were never observed in corresponding regions of control animals (C). Scale bars represent 20 μm (A and B), 10 μm (C), 6 μm (D) and 2 μm (E). (F) As shown here for the CPu of a *ChAT*$^{cre/+}$*;Nkx2-1*$^{fl/fl}$ mouse at 4 weeks of age, the remaining ChAT-ir neurons (in light brown; note dendritic processes) do not express Nkx2-1 (dark brown nuclei). (G–I) Confocal microscopy of double-labelled sections of *ChAT*$^{cre/+}$*;R26R;Nkx2-1*$^{fl/fl}$ mice at 4 weeks of age. As shown for the CPu, double immunofluorescence for β-gal and ChAT demonstrates that the overwhelming majority of the remaining ChAT-ir neurons are positive for β-gal. Scale bars represent 50 μm (F) and 30 μm (G–I).

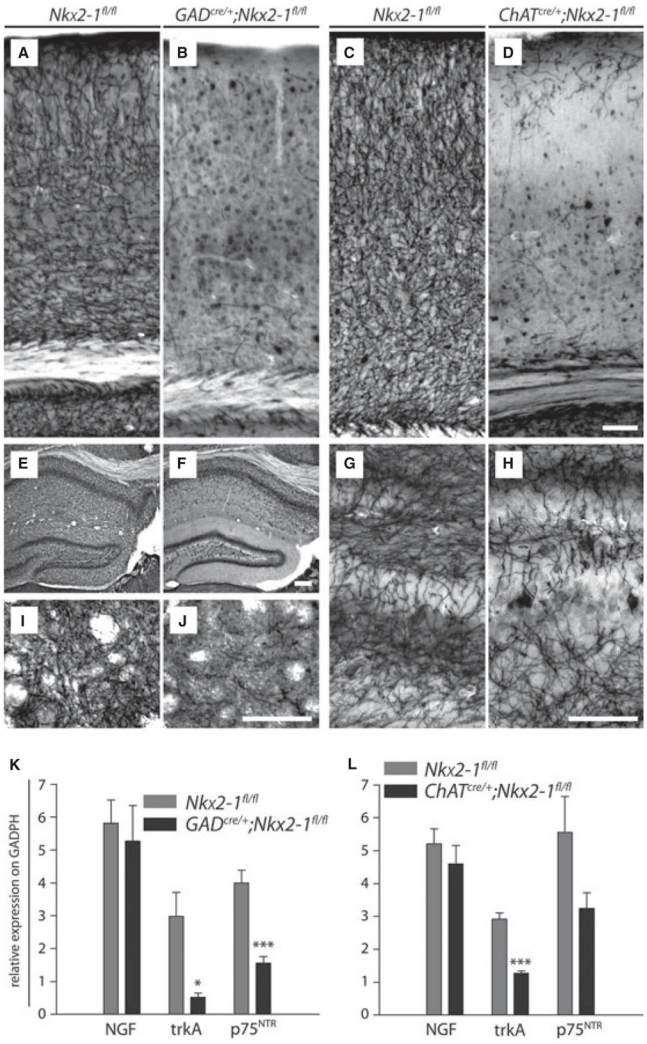

Fig. 5.

Loss of ventral forebrain cholinergic neurons leads to extended target denervation and impaired expression of the neurotrophin receptors *trkA and p75*^{NTR}. (A–J) AChE histochemistry performed for control (A, E, I, C, G, *Nkx2-1*$^{fl/fl}$) and mutant (B, F, J, *GAD*$^{cre/+}$*;Nkx2-1*$^{fl/fl}$; D, H, *ChAT*$^{cre/+}$*;Nkx2-1*$^{fl/fl}$) mice. As shown for the somatosensory cortex (A, C), the hippocampal formation (E, G) and the CPu (I), an intense labelling of fibres was observed in both control strains whereas this staining pattern was largely missing in the neocortical mantle of the two mutants (B, D). In the *GAD*$^{cre/+}$*;Nkx2-1*$^{fl/fl}$ mice, similar observations were made for the dentate gyrus, the hippocampal subfields CA3 and CA1 (F), and the CPu (J). The extent of fibre loss in all parts of the hippocampus of *ChAT*$^{cre/+}$*; Nkx2-1*$^{fl/fl}$ mice was less pronounced. The 'patch-like' defects are shown for the dentate gyrus at higher magnification (H). Scale bars – 100 μm (A–D), 50 μm (E–J). (K, L) Quantification of *NGF*, *trkA* and *p75*^{NTR} expression levels by using quantitative real-time PCR. No significant differences were detected between *GAD*$^{cre/+}$*;Nkx2-1*$^{fl/fl}$ mutants and *Nkx2-1*$^{fl/fl}$ controls as well as *ChAT*$^{cre/+}$*;Nkx2-1*$^{fl/fl}$ mutants and their corresponding *Nkx2-1*$^{fl/fl}$ controls in the levels of *NGF*. A strong reduction was observed for *trkA* transcripts in both *GAD*$^{cre/+}$*;Nkx2-1*$^{fl/fl}$ and *ChAT*$^{cre/+}$*;Nkx2-1*$^{fl/fl}$ mutant mice compared with their controls, whereas the decrease for *p75*^{NTR} was found to be significant only for

GAD$^{cre/+}$;*Nkx2-1*$^{fl/fl}$ mice. Histograms show mean values + SEM. Significance is indicated by asterisks –*$P < 0.01$; ***$P < 0.001$.

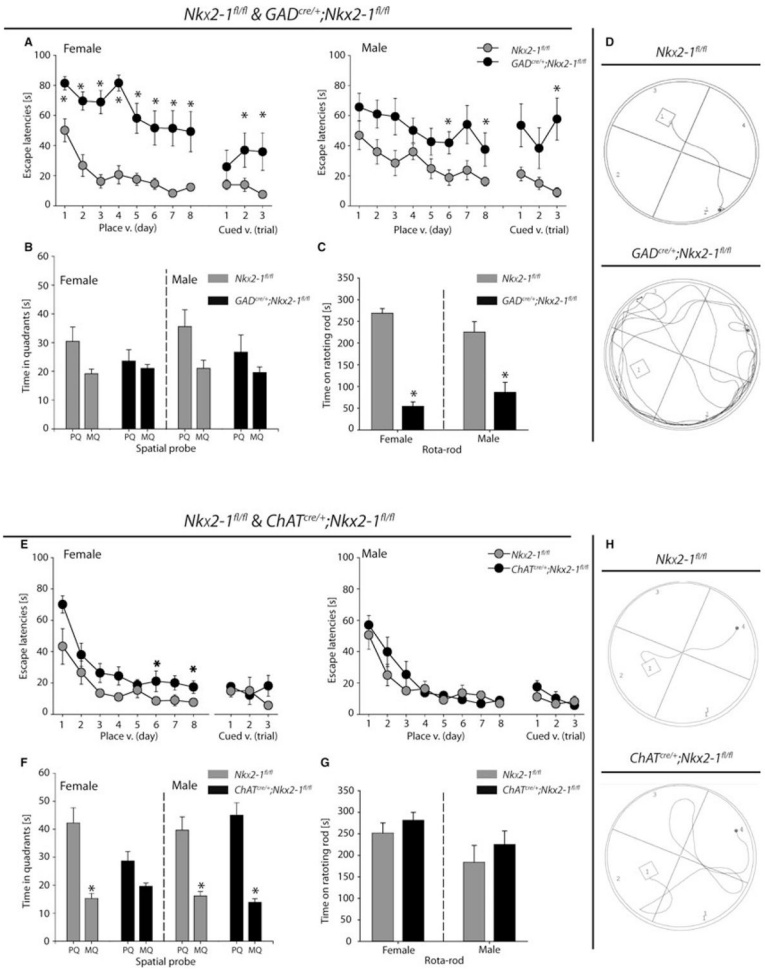

Fig. 6.

Impaired spatial memory and motor deficits in *GAD*$^{cre/+}$*;Nkx2-1*$^{fl/fl}$ mice and learning deficits in female *ChAT*$^{cre/+}$*;Nkx2-1*$^{fl/fl}$ mice. (A) Escape latencies during the place and cued version (v.) of the Morris water maze (MWM) are shown for female and male *GAD*$^{cre/+}$*;Nkx2-1*$^{fl/fl}$ and *Nkx2-1*$^{fl/fl}$ mice. Female and male mutant mice failed to learn the location of the platform. Data are presented as means ± SEM; **P* < 0.05 vs. *Nkx2-1*$^{fl/fl}$. (B) The time (spatial probe of the MWM) spent in the platform quadrant (PQ) and the mean time spent in the three other quadrants (MQ) are presented for female and male *GAD*$^{cre/+}$*;Nkx2-1*$^{fl/fl}$ and *Nkx2-1*$^{fl/fl}$ mice. Female and male mutant mice failed to remember the former location of the platform, but control mice also showed slight deficits in spatial memory. Data are presented as means + SEM. (C) Rota-rod test for female and male *Nkx2-1*$^{fl/fl}$ and *GAD*$^{cre/+}$*;Nkx2-1*$^{fl/fl}$ mice. The time spent on the rotating rod is shown for all mutants in comparison with control mice. Data are presented as mean + SEM; **P* < 0.05 vs. *Nkx2-1*$^{fl/fl}$. (D) Representative paths followed by a female *Nkx2-1*$^{fl/fl}$ control and a female *GAD*$^{cre/+}$*;Nkx2-1*$^{fl/fl}$ mutant mouse on the third day of the place version. (E) Escape latencies during the place and cued version (v.) of the MWM for female and male *Nkx2-1*$^{fl/fl}$ and *ChAT*$^{cre/+}$*;Nkx2-1*$^{fl/fl}$ mice are shown. Female *ChAT*$^{cre/+}$*;Nkx2-1*$^{fl/fl}$ mice needed more time to find the platform than female control mice on days 6 and 8. Data are presented as mean ± SEM; **P* < 0.05 vs. *Nkx2-1*$^{fl/fl}$. (F) The time (spatial probe of the MWM) spent in the platform quadrant (PQ) and the mean time spent in the three other quadrants (MQ) is presented for female and male *Nkx2-1*$^{fl/fl}$ and *ChAT*$^{cre/+}$*;Nkx2-1*$^{fl/fl}$ mice. Only female

mutant mice failed to remember the former location of the platform. No difference in the performance of male *ChAT*$^{cre/+}$;*Nkx2-1*$^{fl/fl}$ and *Nkx2-1*$^{fl/fl}$ mice was detected. Data are presented as mean + SEM; *$P < 0.05$ vs. PQ. (G) The time spent on the rotating rod is plotted on the diagram for female and male *Nkx2-1*$^{fl/fl}$ and *ChAT*$^{cre/+}$;*Nkx2-1*$^{fl/fl}$ mice. No differences between mutants and control mice were detected. Data are presented as mean + SEM. (H) Representative paths followed by a female *Nkx2-1*$^{fl/fl}$ control and a female *ChAT*$^{cre/+}$;*Nkx2-1*$^{fl/fl}$ mutant mouse on day 3 of the place version.

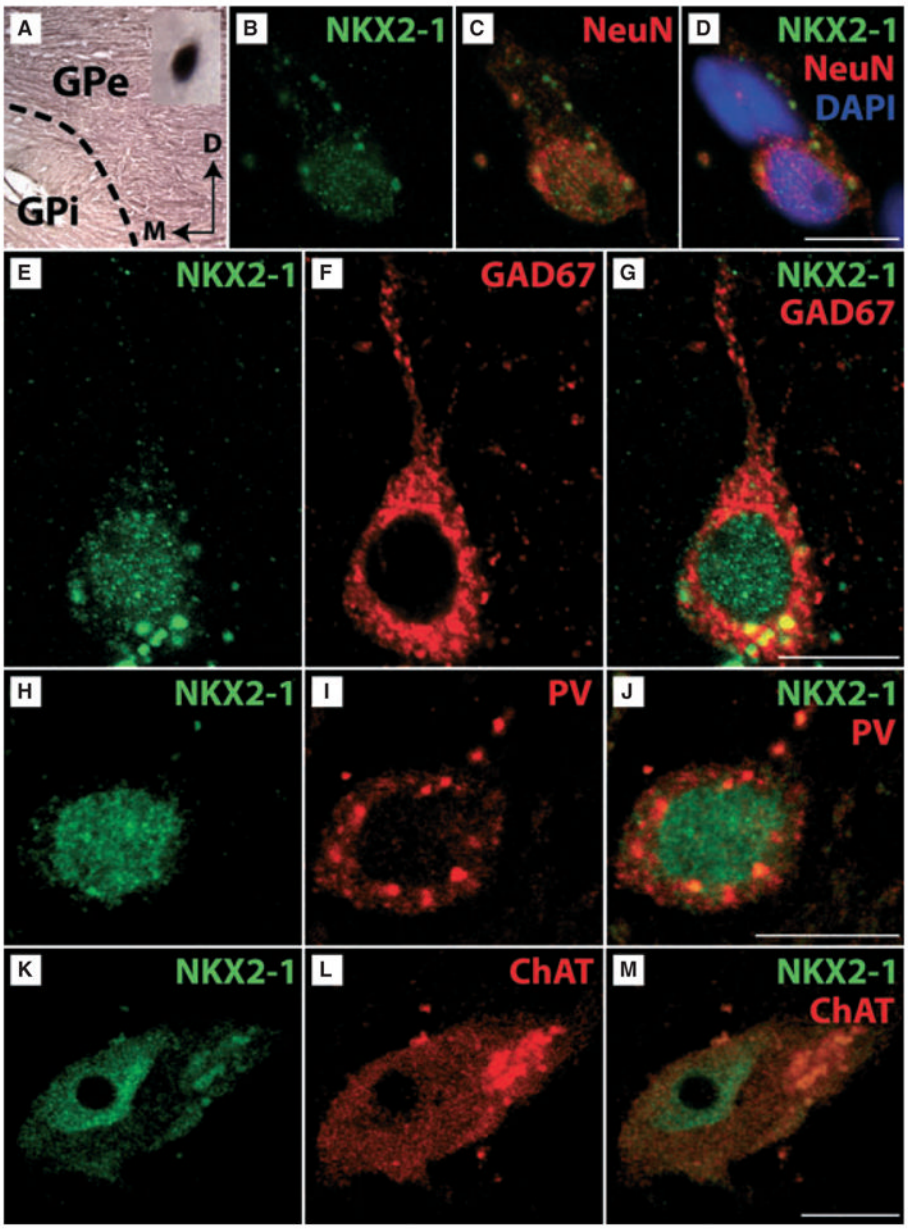

Fig. 7.

Expression of NKX2-1 in the human basal ganglia. (A) IHC for NKX2-1 for a tissue sample of the human globus pallidus is shown (D, dorsal; M, medial) at low magnification. Note that the external part of the globus pallidus (GPe) is more intensively labelled than the internal part (GPi). The dashed line indicates the border between the two compartments of the GP. At high magnification (see inset) a NKX2-1-positive cell profile is shown. (B–D) Triple-staining for Nkx2-1 (B), the neuronal marker NeuN (C), and the nuclear marker DAPI (D) confirmed nuclear expression of NKX2-1 by the neurons. (E–G) Double-labelling for NKX2-1 (E) and GAD67 (F) revealed that NKX2-1 is expressed by GABAergic GPe-neurons (merged, G). Additional double-labellings for NKX2-1 (H) and PV (I) revealed that at least part of these neurons are also immunoreactive for parvalbumin (merged, J). (K–M) Double IHC for NKX2-1 (K) and ChAT (I) revealed that NKX2-1 is expressed by cholinergic neurons mostly located in the putamen bordering the GPe (merged, M). Note

intense fluorescence of lipofuscin particles which are frequently seen in human neurons (see Buhl & Schlote, 1987). Scale bar (for B–M) – 10 μm.

Table 1

Cell counts (mean ± SEM) for ChAT- and PV-immunoreactive neurons in 3-month-old *Nkx2-1$^{fl/fl}$, GAD$^{cre/+}$;Nkx2-1$^{fl/+}$ and GAD$^{cre/+}$;Nkx2-1$^{fl/fl}$* mice obtained by stereological cell counts

	ChAT			PV		
Area	***Nkx2-1$^{fl/fl}$***	***GAD$^{cre/+}$;Nkx2-1$^{fl/+}$***	***GAD$^{cre/+}$;Nkx2-1$^{fl/fl}$***	***Nkx2-1$^{fl/fl}$***	***GAD$^{cre/+}$;Nkx2-1$^{fl/+}$***	***GAD$^{cre/+}$;Nkx2-1$^{fl/fl}$***
MSvBD	1353 ± 363	1360 ± 394	282 ± 73	1096 ± 313	987 ± 284	548 ± 197
hDB-SI	958 ± 219	1070 ± 47	153 ± 107	268 ± 46	243 ± 116	55 ± 27
CPu	6556 ± 1291	5938 ± 564	90.5 ± 72	8030 ± 734	7056 ± 293	552 ± 144
LGP	1177 ± 215	1209 ± 64	557 ± 137	1881 ± 216	1875 ± 164	419 ± 201

Table 2

Cell counts (mean ± SEM) for ChAT-ir neurons in P15, 3-month- and 6-month-old *Nkx2-1$^{fl/fl}$ and ChAT$^{cre/+}$;Nkx2-1$^{fl/fl}$* mice obtained by stereological cell counts

	P15		3 months old		6 months old	
Area	***Nkx2-1$^{fl/fl}$***	***ChAT$^{cre/+}$;Nkx2-1$^{fl/fl}$***	***Nkx2-1$^{fl/fl}$***	***ChAT$^{cre/+}$;Nkx2-1$^{fl/fl}$***	***Nkx2-1$^{fl/fl}$***	***ChAT$^{cre/+}$;Nkx2-1$^{fl/fl}$***
MSvBD	1899 ± 430	2085 ± 333	1585 ± 354	790 ± 158	1812 ± 241	1155 ± 204
hDB-SI	956 ± 104	966 ± 176	1236 ± 282	675 ± 155	1185 ± 66	615 ± 208
CPu	6995 ± 630	6990 ± 1019	6742 ± 947	3187 ± 456	6646 ± 425	4077 ± 379
LGP	1199 ± 44	1222 ± 229	1109 ± 189	419 ± 190	1065 ± 102	487 ± 135